





Review

Cost Efficiency Analysis of H₂ Production from Formic Acid by Molecular Catalysts

Maria Solakidou ¹, Aikaterini Gemenetzi ¹, Georgia Koutsikou ¹, Marinos Theodorakopoulos ¹, Yiannis Deligiannakis ² and Maria Louloudi ^{1,*}

¹ Laboratory of Biomimetic Catalysis & Hybrid Materials, Department of Chemistry, University of Ioannina, 45110 Ioannina, Greece

² Laboratory of Physical Chemistry of Materials & Environment, Department of Physics, University of Ioannina, 45110 Ioannina, Greece

* Correspondence: mlouloud@uoi.gr

Abstract: The development of low-carbon technologies that will facilitate the efficient use of hydrogen (H₂) as an energy carrier is a critical requirement of contemporary society. To this end, it is anticipated that the cost of H₂ production will become a key factor *in tandem* with production efficiency, process safety, and transport. Much effort has been made to create and develop new, reversible, and sustainable H₂ storage systems. Among current techniques, formic acid (FA) has been identified as an efficient energy carrier for H₂ storage. Numerous homogeneous catalysts based on transition metals with high activity and selectivity have been reported for selective FA dehydrogenation. In this review, we outline the recent advances in transition-metal molecular catalysts for FA dehydrogenation. Selected catalytic systems that could be implemented on an industrial scale and considered potential materials in fuel cell (FC) technology have been cost-evaluated. We highlight some critical engineering challenges faced during the technology's scale-up process and explain other factors that are frequently ignored by academic researchers. Finally, we offer a critical assessment and identify several system limitations on an industrial scale that are currently impeding future implementation.

Keywords: hydrogen production; cost analysis; formic acid dehydrogenation; metal precursor; ligand; additive; solvent



Citation: Solakidou, M.; Gemenetzi, A.; Koutsikou, G.; Theodorakopoulos, M.; Deligiannakis, Y.; Louloudi, M. Cost Efficiency Analysis of H₂ Production from Formic Acid by Molecular Catalysts. *Energies* **2023**, *16*, 1723. <https://doi.org/10.3390/en16041723>

Academic Editor: Asif Ali Tahir

Received: 17 January 2023

Revised: 2 February 2023

Accepted: 4 February 2023

Published: 9 February 2023



Copyright: © 2023 by the authors. Licensee MDPI, Basel, Switzerland. This article is an open access article distributed under the terms and conditions of the Creative Commons Attribution (CC BY) license (<https://creativecommons.org/licenses/by/4.0/>).

1. Introduction

The fast growth of the economy and technology has provoked severe energy and environmental issues. Energy consumption in the transportation sector climbed dramatically from 23% to 29% in 30 years. During this period, the global demand for primary energy grew by a factor of 2.5, from 5519 Mtoes to 13,972 Mtoes [1]. The Intergovernmental Panel on Climate Change (IPCC) determined that, in order to restrict the rise in global temperature to 1.5 °C, global net anthropogenic CO₂ emissions must reach net zero by around 2050 (IPCC, 2018) [2]. The European Union is aiming to achieve net zero emissions by 2050 and other countries are likely to follow suit [2]. In the context of the energy transition, hydrogen (H₂) represents a very promising candidate. There are several potential routes for H₂ production in energy systems, some of which are currently being implemented in actual projects [3]. H₂ may be used in industrial processes (synthesis of fuels, chemicals, etc.), transport, and building heating systems. So far, the major H₂ usage pathways are summarized in Figure 1 and discussed in depth in the literature [4,5]. H₂ use presents many advantages. For example, it is not only the most plentiful chemical element in the universe, but its utilization also produces no greenhouse gas emissions and just water as a byproduct [6]. Its energy-storage capacity is an additional benefit, as 1 kg of H₂ may produce about 120 MJ (=33.33 kWh) of energy, which is three times that of ordinary diesel, four times that of coking coal, and six times that of coal [7].

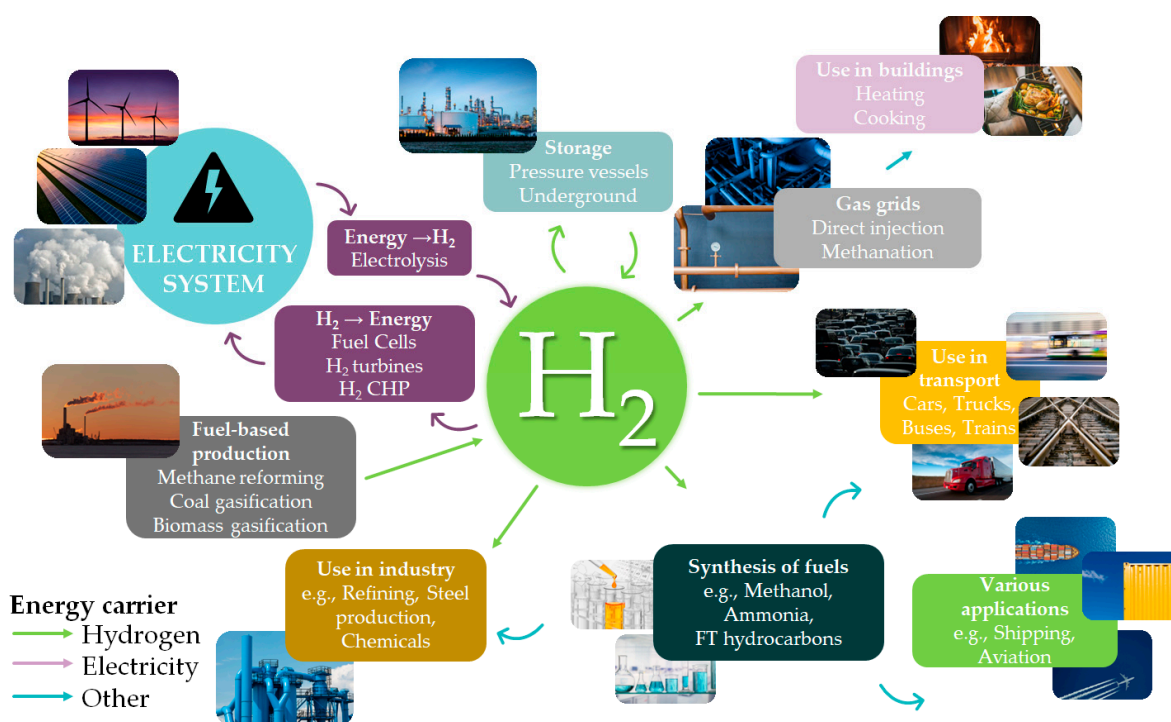


Figure 1. H₂ production and usage pathways.

These characteristics make H₂ an attractive transportation fuel. It can be used as fuel in an internal combustion engine or provide the electrical power for an electric car fuel cell. Within this context, H₂ is viewed as a potential low-carbon fuel for long-distance transportation modes, such as trucks, rail, and shipping [8]. Compared to battery-powered electric vehicles, H₂-powered passenger vehicles might cover longer driving ranges, with shorter refueling periods and, in certain circumstances, reduced ownership costs [9]. There are more than 350 H₂ fueling stations in North America, Europe, Asia, and Oceania [10]. Numerous cities throughout the world, including those in the United States, Japan, China, and Europe, employ hydrogen buses [11]. Alstom has created a hydrogen-powered train, the first of which entered service in 2018 in Germany and this year has traveled without refueling 1175 km [12]. In the context of a forthcoming wide use of H₂, the development of H₂ infrastructure and technologies is often assessed taking into consideration larger economic development goals, too.

Up to now, the most common method for H₂ production is from fossil fuels, such as natural gas reforming (Grey Hydrogen) and coal gasification (Black Hydrogen), (Figure 2a) [13]. Water electrolysis as a H₂ source (Yellow Hydrogen) has been used in specific industrial applications for more than a century. Its popularity has increased in recent decades due to the need for environmentally friendly energy technologies using renewable energy sources (Green Hydrogen). However, the main limitation of its use remains its high cost of 3.6–5.1 \$/kg H₂ [14]. Natural gas reforming combined with CO₂ capture and storage (Blue Hydrogen) is considered the most appealing alternative for a carbon-free technology at a reasonable price (Figure 2a) [15].

Regarding H₂'s development as an energy source, there are hindrances due to some of its physical properties, such as its very low volumetric energy density. At standard temperature and pressure (STP), the volumetric energy density of gasoline is 32 MJ/L, whereas that of H₂ is just 0.01 MJ/L [16]. This makes it challenging to obtain effective H₂ storage at ambient conditions. According to the U.S. Department of Energy (DOE) standards, the ultimate goal for the gravimetric and volumetric H₂ onboard storage capacities is 0.065 kg H₂/kg and 0.050 kg/L, respectively [17]. To accomplish this goal, several technologies for effective large-scale H₂ storage are being employed (Figure 2b), all presenting advantages and drawbacks. For example, H₂ storage in high-pressure compressed gas cylinders or

cryogenic liquid tanks is an option, but it has significant energy losses (H_2 compression, liquefaction, and boil-off), as well as a low volumetric energy capacity [18]. The energy density of state-of-the-art onboard H_2 storage (700 bar) is 1.9 kWh/kg and 1.4 kWh/L, which corresponds to 5.7 wt% H_2 [4]. To circumvent the limits of these conventional techniques, both physisorption in porous materials and chemical storage approaches have been developed [19]. Physisorption's benefits include rapid kinetics, full reversibility, and great activity. Nevertheless, due to the weak van der Waals interactions between H_2 gas and the examined materials [20], adequate storage capacities are often achieved at low temperatures and/or high pressures, increasing the overall cost of the procedure.

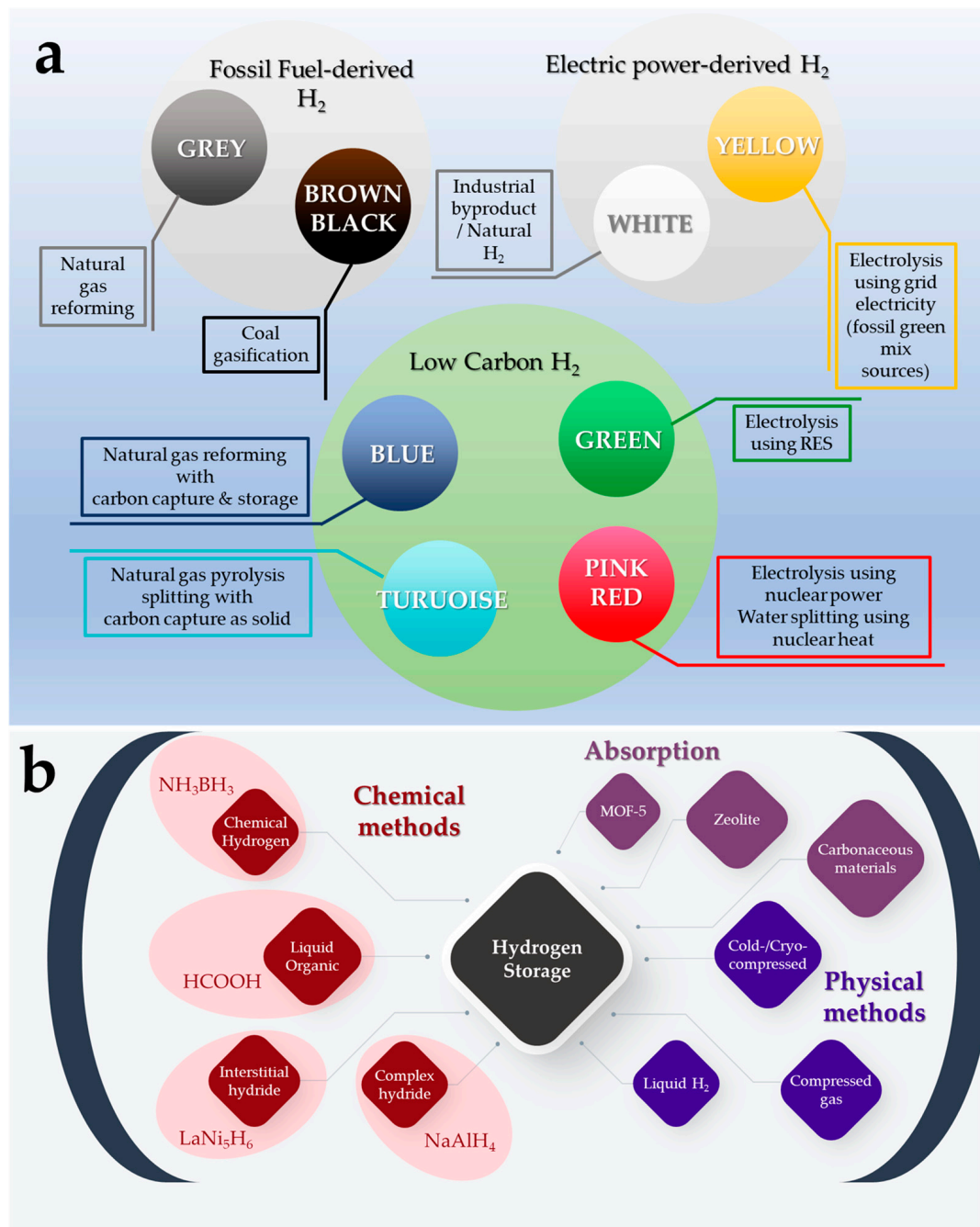


Figure 2. (a) Color classification of H_2 based on the means of production (b) Hydrogen storage methods.

Chemical hydrogen storage in solid carriers, such as metal hydrides, and in liquid carriers, e.g., (organic) hydrogen carriers (LOHCs), provides the potential benefits of increased safety, convenience, volumetric energy efficiency, and potential ease of use. The latter may be easily dispensed using infrastructure similar to today's gasoline refueling stations, which makes them of significant interest for transportation applications [21,22]. Among LOHCs, formic acid (FA, HCOOH) has received considerable interest due to its relatively high volumetric energy density (6.36 MJ/L), low toxicity, and low flammability, establishing a safe H₂ carrier option [23]. The dehydrogenation (decarboxylation) of HCOOH is accompanied by a low reaction enthalpy (31.2 KJ/mol) in the majority of systems. Hence, H₂ may be generated at ambient conditions, which would be within the DOE's objective [24]. Towards this direction, numerous transition-metal-based homogeneous and heterogeneous catalysts with high activity have been reported for FA dehydrogenation [25].

Within the context of in situ H₂ production by catalytic FA dehydrogenation and its potential implementation, in the present review, FA as a liquid organic H₂ carrier and the cost of various molecular catalytic systems are evaluated. Those systems could be applied on an industrial scale and are considered potential candidates for use in fuel cell (FC) technology. A future potential implementation is described as a function of three main features: efficiency, cost, and scalability. The cost analysis included herein is based on the current cost of the metal precursor, ligand, additive, and solvent. Moreover, we highlight some critical engineering challenges faced during the technology's scale-up application, identifying several system limitations on an industrial level that are currently impeding future implementation.

2. Formic Acid: An Efficient Liquid Carrier for H₂ Storage

FA's high density (1.22 g cm³) translates into a volumetric H₂ concentration of 53 g H₂/L, which is equivalent to 1.77 kWh L⁻¹. This surpasses the industry standards of the Toyota Mirai (700 bar H₂ storage tank with 1.4 kWh L⁻¹), which consumes 0.76 kg H₂/100 km [26,27]. Despite the advent of electricity-driven technologies and the manufacturing of FA from green feedstock, the FA market is still restricted until new breakthroughs impose its broader commercialization [28]. FA, a typical industrial reagent, is non-flammable, non-toxic, simple to handle at room temperature, and does not require high-pressure storage or a catalytic reforming unit. It is one of the most widely used organic chemical raw ingredients in the pesticide, leather, dyes, medicine, and rubber sectors [29]. FA supplied at a concentration of 85% is the worldwide industry standard, while 99% is required for particular applications [30]. The global output of FA ranged from 750,000 to 800,000 tons between 2014 and 2019, with the price being \$400/ton. The Global FA Market was worth 756.5 million \$ in 2018 and is projected to reach 828.1 million \$ by the end of 2025, expanding at a CAGR (compound annual growth rate) of 1.3% between 2018 and 2025 [29]. The reduced labor and capital costs, along with the constantly expanding market, will enable China to boost its FA production capacity, making it the leading producer and exporter of FA [28].

Regarding the involvement of FA in energy issues, FA decomposition occurs via the two routes, as depicted in Figure 3a. The first equation describes HCOOH dehydrogenation into H₂ and CO₂, whereas in the second one, HCOOH dehydration provides H₂O and CO, which is responsible for the inactivation of fuel cell electrodes. Both reactions are dependent on the employed catalysts, the temperature, and the concentration of FA [31]. Using an appropriate catalyst at low temperatures, both the dehydrogenation of FA (FADH) to CO₂ and the hydrogenation of CO₂ to FA (FAH) are possible, resulting in a "carbon-neutral cycle" (See Figure 3b) [32].

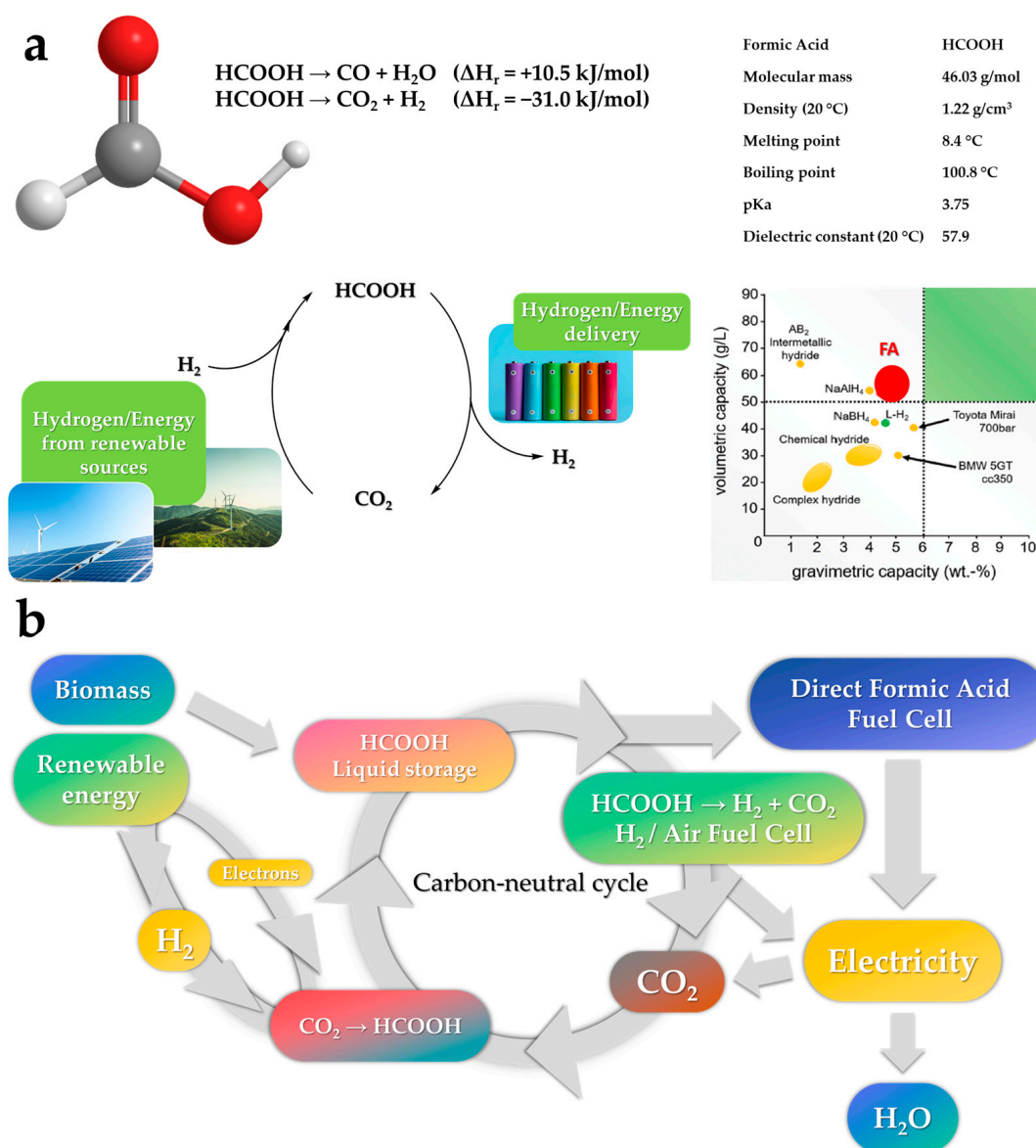


Figure 3. (a) FA properties and decomposition reactions (b) Cycle of FA dehydrogenation and regeneration by CO₂ hydrogenation.

CO₂ hydrogenation to FA is a crucial challenge targeting a double benefit for the planet since it prevents environmental pollution caused by CO₂ emissions from industrial effluents and, at the same time, it regenerates a substantial organic feedstock. A carbon-neutral H₂ storage/release cycle is feasible and it consists of the quantitative hydrogenation of CO₂ to form FA, followed by its selective dehydrogenation [23]. Up-to-day, dehydrogenation of FA, using a molecular catalyst, has gained a lot of interest in the research community, due to its higher performance in mild conditions vs. the hydrogenation path [20]. Based on this potential, it is possible to envision automotive applications in which gasoline is substituted by FA and automobiles are equipped with technology based on fuel cells; either direct formic acid fuel cells (DFAFC) [33] or hydrogen fuel cells (HFC) such as PEMFCs (Proton-exchange membrane fuel cells) [26].

DFAFCs are advantageous for compact portable HFC applications and promising for automotive batteries of electric vehicles. They offer the potential for a carbon-neutral cycle in which CO₂ is collected and subsequently electrolyzed to produce FA. Although DFAFCs conversion of FA to electricity seems to be simple, their performance is restricted by fuel crossover and anode catalyst poisoning [34]. PEMFCs, on the other hand, are

well-established for use in electric vehicles, with maximum power density higher than DFAFCS, i.e., 1400–2000 mW/cm² [35] vs. 550 mW/cm² [36] (Figure 4).

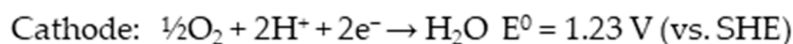
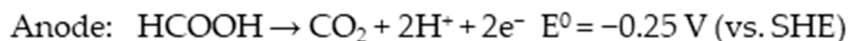
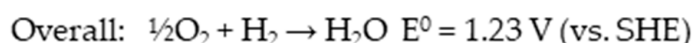
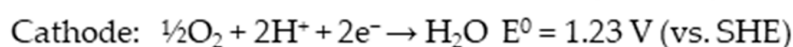
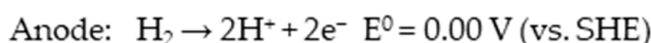
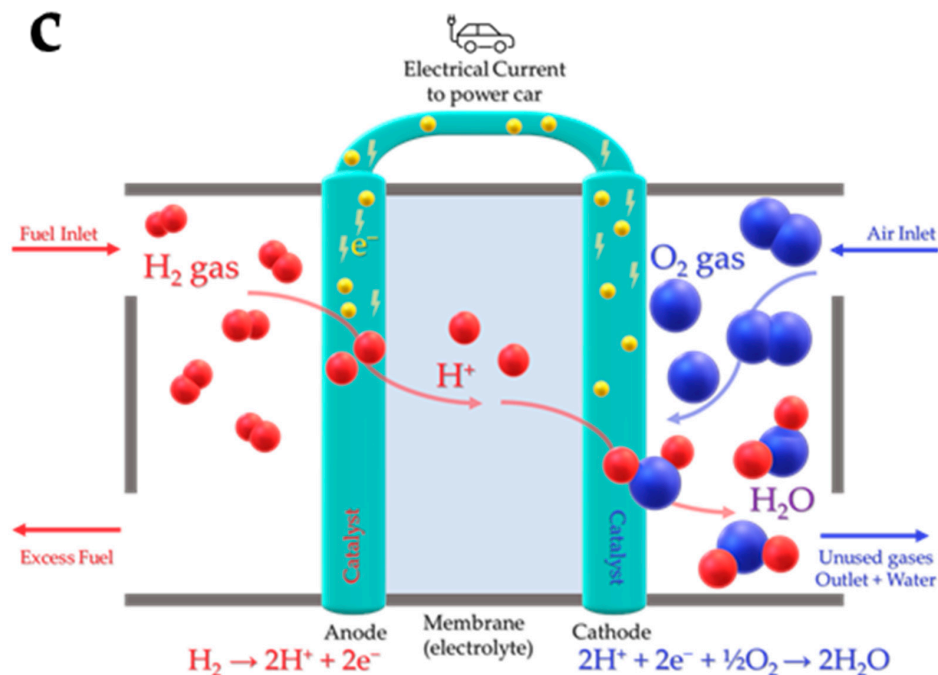
a**DFAFCs****b****PEMFCs****c**

Figure 4. The reactions that occur at the anode and cathode of (a) Direct Formic Acid Fuel Cells (DFAFC), (b) Proton-exchange membrane fuel cells (PEMFC), (c) Schematic representation of a PEMFC.

An efficient catalyst for H₂ generation to be used in PEMFC must meet the following requirements: selectivity, high stability (TON), high activity (TOF), and low cost [37]. In order to obtain customer acceptance of a new technology, economic factors are of paramount significance. Huang recently evaluated eight homogenous systems which rely on the use of two dimension-free equations, CON (Catalyst cost normalized to the TON value) and COF (Catalyst cost normalized to the TOF value) [37] (Figure 5). In this methodology, it is proposed that for a catalyst to be considered valuable for use in automobile applications, it should have a maximum CON and COF value of 0.35 [37], a range of TOF between 5000 to 10,000 h^{−1}, and TON in the order of multi-millions [38]. The same research group, in another perspective, enrich their methodology with a life cycle assessment (LCA) data analysis of FA with CO₂ capture and storage (CCS) and CO₂ capture and utilize prospects (CCU) [23]. As depicted in Figure 5, the set thresholds for a product (H₂ in this example)

and the overall reactor system (tank, converter, controller) allow for a comparison of the economic viability of new technologies to those now in use. For each process, there exists a region in the CON/COF diagram where catalyst costs satisfy the corresponding cost threshold requirements. Catalysts with greater CON or COF values result in a higher-than-desired product cost ($CON > CON^0$) or system cost ($COF > COF^0$). Consequently, the green region in the diagram denotes the aim for catalysts that economically meet all the required criteria.

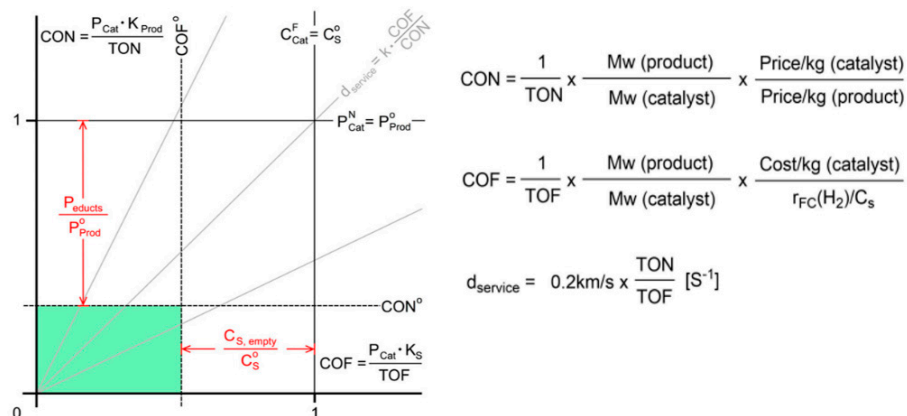


Figure 5. Margins of catalyst price normalized vs. TON (CON) or TOF (COF). According to cost-analysis methodology, “product” refers to the total cost of all raw materials, while C_s is the system expenses without a catalyst (e.g., fuel tank, pumps, FA converter, and controller). Adapted from [37] with permission.

Moreover, to determine how close a technology is to operational deployment and to evaluate the development status of emerging technologies, the U.S. Department of Defense and Horizon 2020 proposed the TRL definition (see Figure 6) [39,40]. Based on this technological assessment, the scale-up implementation of some homogeneous catalysts for the majority of FA-to-power technologies ranges between TRL 7 and TRL 8 [30,41–43]. However, for these systems to be applied in a real operational environment [TRL 9], a lot of further improvement is needed as the requirements for this level take into consideration the catalytic activity in tandem with the decrease of the cost.

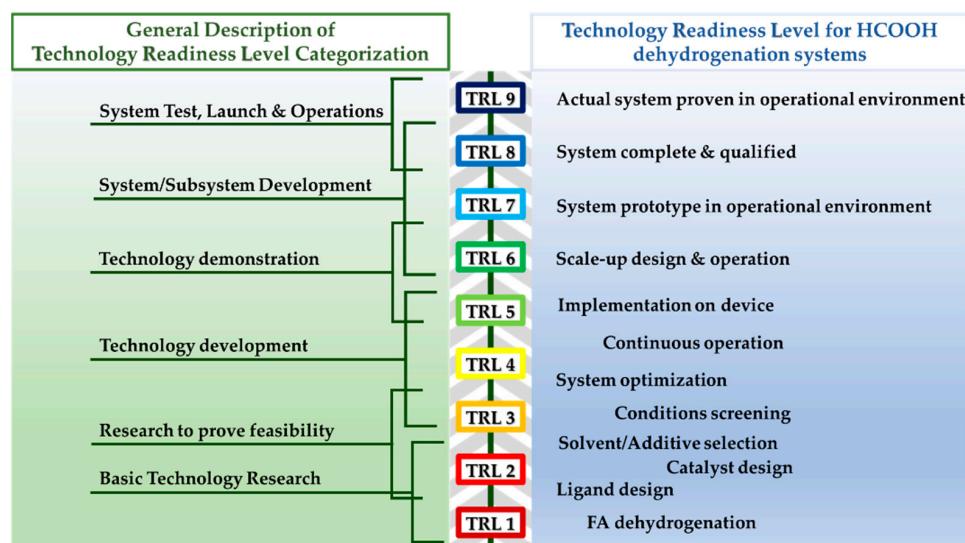


Figure 6. Technology Readiness Levels (TRL) for FA dehydrogenation catalytic systems.

3. Description of Our Cost Analysis Methodology: Lab-Scale and Industrial-Scale Price

Considering the scarcity of published data in the literature, regarding the contribution of metal precursor, ligand, additive, and solvent to the final expenditures of a given apparatus for the catalytic H₂ production from molecular catalysts, our cost analysis is based on two steps. First, a “lab-scale” price estimation is performed, based on prices for the components, where the price-per-unit (kg or L) is taken from the websites of some reference chemical supply companies, such as Sigma-Aldrich, Thermo Scientific, TCI Chemicals, and others. In Table 1, we present a lab-scale cost estimate of typical metal precursors, for selected systems. In Table 2, lab-scale cost estimates for pertinent ligands are presented. An indicative “industrial scale” cost estimate is compiled by introducing a “scale-factor” that can divide the cost. Typically, this factor is in the order of 10. Some critical engineering challenges faced during the technology’s scale-up are (a) the efficiency (TONs = stability and TOFs = activity, [44]) (b) the cost (\$/kg or \$/mol) (Figure 7), and (c) the eco-impact or ecological footprint. Herein, we focus on the catalyst production cost, originating from:

$$[\text{Cost of a catalytic system}] = \frac{\{\text{cost of [metal precursor]} + [\text{ligand}] + [\text{solvent}] + [\text{additives}]\}}{\{\text{kg of Hydrogen produced by that catalyst}\}} \quad (1)$$

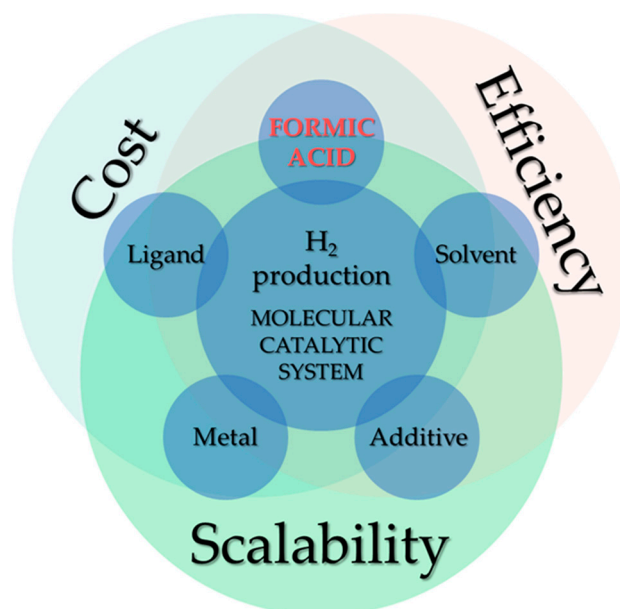


Figure 7. Major factors that determine the techno-economic profile of a FA dehydrogenation catalytic system.

This could be expressed using the following equations:

$$\text{Cost} = \frac{\$}{\text{kg}_x} \text{ (price provided by companies), where } x = \text{metal precursor, ligand, additive, solvent} \quad (2)$$

$$\text{Efficiency} = \frac{\text{kg H}_2}{\text{kg}_x}, \text{ where kg H}_2 \text{ is calculated from TON} \quad (3)$$

$$\text{Scalability} = \sum_{x=1}^{x=4} \frac{\$}{\text{kg}_x} = \$/\text{kg H}_2, \text{ } x_1 = \text{metal precursor, } x_2 = \text{ligand, } x_3 = \text{additive, } x_4 = \text{solvent} \quad (4)$$

The ecological footprint is of great importance. However, its analysis is out of the scope of the present review. There are numerous comprehensive articles where the ecological impact of fossil-based FA strategies with LCA is discussed [23]. Herein, high-performing catalytic systems have been selected, i.e., with TONs in the range of 103–106, as viable case studies for implementation in industrial use. Thus, the present review is organized

as follows: we analyze the efficiency (kg H₂ per kg_{xi}) in tandem with cost (\$/kg H₂) according to x_1 = metal precursor (Section 3.1), x_2 = ligand (Section 3.2), x_3 = additives (Section 3.3), x_4 = solvent (Section 3.4). This analysis is based on selected catalytic systems in the literature, which show relatively high TONs and TOFs. In Section 4, we make an overall-cost evaluation, offering a critical assessment and identifying several system limitations on an industrial scale that are currently impeding future implementation.

3.1. Catalytic Metals in FA Dehydrogenation

The use of transition metals in catalysis for transformations of organic molecules is well-established in both academia and industry and well-recognized by Nobel prize awards in related fields. It is known that precious metals, such as Ru, Ir, and Rh, can be involved in a plethora of catalytic transformations, among them de-hydrogenation and/or hydrogenation reactions, due to their ability to assist in 2e-redox processes and to form reactive metal hydride complexes [45]. To this front, many transition metal hydrides, as critical intermediates in proton and hydride transfer catalytic steps, are combined with phosphines which are 2e-ligands of medium hardness and with a π -acceptor ability [45,46].

Within this context, since 1967, H₂ production from FA has been studied mostly using noble metal catalysts, such as Ir, Ru, and Rh [47] (Figure 8). The activity, productivity, and selectivity of catalysts based on noble metals, e.g., Ir-phosphine and Ru-phosphine complexes, has greatly increased in the following decades. In 1998, Puddephat et al. made considerable progress by introducing a binuclear Ru-phosphine complex [Ru₂(-CO)(CO)₄(-dppm)₂] with a TOF~500 h⁻¹, operating at room temperature [48]. Up to 2008, progress on the survey for FA dehydrogenation as a potential H₂ storage carrier was rather slow. Then, the groups of Beller and Laurentzy investigated various combinations of Ru metal precursors with phosphine ligands, realizing the need for additives, mainly amines.

ELIGIBLE CATALYTIC METALS FOR HOMOGENEOUS FA DEHYDROGENATION																	
19 K Potassium Alkali Metal	20 Ca Calcium Alkaline Earth Metal	21 Sc Scandium Transition Metal	22 Ti Titanium Transition Metal	23 V Vanadium Transition Metal	24 Cr Chromium Transition Metal	25 Mn Manganese Transition Metal	26 Fe Iron Transition Metal	27 Co Cobalt Transition Metal	28 Ni Nickel Transition Metal	29 Cu Copper Transition Metal	30 Zn Zinc Transition Metal	31 Ga Gallium Post-Transition Metal	32 Ge Germanium Metalloid	33 As Arsenic Metalloid	34 Se Selenium Metalloid	35 Br Bromine Halogen	36 Kr Krypton Noble Gas
37 Rb Rubidium Alkali Metal	38 Sr Strontium Alkaline Earth Metal	39 Y Yttrium Transition Metal	40 Zr Zirconium Transition Metal	41 Nb Niobium Transition Metal	42 Mo Molybdenum Transition Metal	43 Tc Technetium Transition Metal	44 Ru Ruthenium Transition Metal	45 Rh Rhodium Transition Metal	46 Pd Palladium Transition Metal	47 Ag Silver Transition Metal	48 Cd Cadmium Transition Metal	49 In Indium Post-Transition Metal	50 Sn Tin Post-Transition Metal	51 Sb Antimony Metalloid	52 Te Tellurium Metalloid	53 I Iodine Halogen	54 Xe Xenon Noble Gas
55 Cs Cesium Alkali Metal	56 Ba Barium Alkaline Earth Metal		72 Hf Hafnium Transition Metal	73 Ta Tantalum Transition Metal	74 W Tungsten Transition Metal	75 Re Rhenium Transition Metal	76 Os Osmium Transition Metal	77 Ir Iridium Transition Metal	78 Pt Platinum Transition Metal	79 Au Gold Transition Metal	80 Hg Mercury Transition Metal	81 Tl Thallium Post-Transition Metal	82 Pb Lead Post-Transition Metal	83 Bi Bismuth Metalloid	84 Po Polonium Metalloid	85 At Astatine Halogen	86 Rn Radon Noble Gas

Figure 8. Eligible metals as catalysts for FA dehydrogenation. Noble metals = Ru, Rh, Ir. Non-noble metals = Mn, Fe, Co, Ni.

Thus, since then, by including additives as cocatalytic agents, highly performing catalysts have been developed, such as [RuCl₂(benzene)]₂/1,2-bisdiphenylphosphinoethane (dppe) [49] and [Ru(H₂O)₆](tos)₂/TPPTS (TPPTS = meta-trisulfonated triphenylphosphine) [50] achieving a TON > 1,000,000 and 20,000 respectively. Filonenko et al. created an efficient catalyst for FA dehydrogenation (T = 90 °C) using a Ru-PNP complex in DMF solvent and DBU additive. Under these conditions, a cyclic operation of the catalyst in both dehydrogenation and hydrogenation reactions is realized, culminating in TONs > 706,500 [51]. Efforts for the development of Ru homogeneous catalysts continue until today with great progress [52–54].

Since the pioneering work of Himeda, [55] in 2009, whose group reported a Cp*Ir catalyst with a 4,4-dihydroxy-2,2-bipyridine ligand, a lot of research activity has been reported in the field of Ir complexes. Ir complexes' price is higher in comparison to Ru analogues; however, their performance is far superior. In this direction, the research group of Li synthesized Ir-based complexes with N,N'-diimine ligands with a TOF value of 487,500 h⁻¹ at 90 °C, which is the greatest TOF recorded up to date [44]. Subsequently, many other publications on the synthesis of Ir catalysts have been published [56–58]. Some reports include the activity of an Ir catalyst coordinated by an N,N'-bidentate ligand in

water without additives [56]. Himeda et al. [57] developed a novel imidazoline-based ligand by combining dihydroxy-pyrimidine with Ir achieving a TOF of $322,000 \text{ h}^{-1}$ and a TON of 2,050,000 under continuous operation. In another work, Himeda et al. [58] showed that an Ir-4DHBP complex at 80°C yielded a maximum gas pressure of 123 MPa, with a CO concentration of $<6 \text{ ppm}$. As a substrate, they used industrial-grade FA (purity $< 85\%$), providing a TON of 5,000,000 and H_2 gas $> 120 \text{ L}$, with a duration of more than 3.5 months [58]. Concerning the Ir-based catalysts, a few recent works can also be included, such as Fischmeister et al. [59], He and Yi et al. [60], and Li et al. [61], albeit with lower H_2 -production yields.

Rh complexes have not been as thoroughly investigated in the catalytic dehydrogenation of FA as their Ru and Ir counterparts, owing to their low stability and activity [46]. Nevertheless, a number of intriguing mechanistic investigations on Rh complexes have been reported. Significant examples include a cyclometalate, $\text{Rh}^{\text{I}}\text{-PN}(\text{C})$ [62], a $[\text{Cp}^*\text{Rh}(\text{dpm})\text{Cl}]\text{Cl}_2$ [63], and a $[(\text{CNC})\text{MesRh}(\text{PMe}_2\text{Ph})]\text{PF}_6$ [64] complex. Despite the far lower performance of Rh catalysts compared with Ru and Ir, Rh is NMR active, offering a viable tool for mechanistic studies [63].

In Table 1, we compile a lab-scale cost-estimate of typical metal precursors for selected systems. In Table 2, the lab-scale cost estimate for pertinent ligands is presented. According to Table 1, the cost of metal makes an important contribution to the overall cost of the system. This cost may be affected by the metals' relative abundance as well as the type of precursor. The relative abundance of metals in the earth's crust vs. cost ($\$/\text{kg}$ metal precursor) is presented in Figure 9. Obviously, noble metal precursors are at least 10-fold more expensive, e.g., $[\text{Fe}(\text{BF}_4)_2] \cdot 6\text{H}_2\text{O} = 4176 \text{ } \$/\text{kg}$ vs. $\text{RuCl}_3 \cdot 3\text{H}_2\text{O} = 16,500 \text{ } \$/\text{kg}$. Although Ru, Ir, and Rh have a similar abundance in earth minerals ($\sim 10^{-3} \text{ mg/kg}$), $\text{IrCl}_3 \cdot 3\text{H}_2\text{O}$ costs $78,000 \text{ } \$/\text{kg}$ vs. $\sim 16,500 \text{ } \$/\text{kg}$ for the $\text{RuCl}_3 \cdot 3\text{H}_2\text{O}$. It is worth mentioning that binuclear metal precursors, used in most cases for synthesizing pincer type and N-donor bidentate ligands have a higher price than mononuclear, following the order: $[\text{Cp}^*\text{RhCl}_2]_2 > [\text{Cp}^*\text{IrCl}_2]_2 > [(\text{C}_6\text{Me}_6)\text{RuCl}_2]_2 > [\text{Ir}(\text{coe})_2\text{Cl}]_2 > [\text{RuCl}_2(\text{benzene})]_2$. Among those, the very common $[\text{Cp}^*\text{IrCl}_2]_2$ metal precursor, used for synthesizing 'half-sandwich' complexes, participates in very efficient catalytic systems with TONs in the order of 10^6 [44,65], (see Table 2, classification according to ligand). The most expensive, but less stable catalytic system is the $[\text{Cp}^*\text{RhCl}_2]_2$ metal precursor with $592,000 \text{ } \$/\text{kg}$.

However, the need for inexpensive and earth-abundant non-noble metal catalysts triggered the development of such systems for H_2 production from FA dehydrogenation. The use of 3d metals is more prevalent in sustainable catalysis than their heavier homolog 4d/5d metal complexes [66] because of their lower cost, reduced toxicity, and, as already mentioned, their greater abundance in the earth's crust. However, first-row transition metals are prone to 1e-transfer processes, often limiting the catalytic efficiency. Appropriate metal-ligand cooperativity could overcome this shortcoming [67]. Undoubtedly, there are known 3d metal complexes with various σ -donor ligands having satisfactorily catalyzed FA dehydrogenation that was once limited to precious metals. The most investigated complexes under this category include mostly Fe-centered catalysts [68–71], while in the last years, a lot of effort has been made in designing new complexes containing Mn [72,73], Ni [74,75], or Co [76] analogues. When we examine non-noble metals and high efficiency in tandem with relatively low prices, the most cost-efficient is a Fe-pincer complex (TONs $> 983,642$), at $\sim 5900 \text{ } \$/\text{kg}$ and $3279 \text{ } \$/\text{kg}$ for the FeBr_2 and FeCl_2 precursors, respectively. $\text{Fe}_3(\text{CO})_{12}$, albeit more costly ($8903 \text{ } \$/\text{kg}$), presents a lower performance with $0.5 \text{ kg H}_2/\text{kg}_{\text{metal precursor}}$. $[\text{Fe}(\text{BF}_4)_2] \cdot 6\text{H}_2\text{O}$, which was used by Boddien et al. [70], has a low cost with $4176 \text{ } \$/\text{kg}_{\text{metal precursor}}$, giving a value of $0.76 \text{ } \$/\text{kg H}_2$. Other non-noble metal precursors, e.g., $\text{BrMn}(\text{CO})_5$ and $\text{NiBr}_2(\text{dme})$, are more expensive with a price between $45,000 \text{ } \$/\text{kg}$ and $27,000 \text{ } \$/\text{kg}$. Their low catalytic efficiency ($1.38 \text{ kg H}_2/\text{kg}_{\text{metal precursor}}$ and $4.06 \text{ kg H}_2/\text{kg}_{\text{metal precursor}}$, Entry, #20, #21 in Table 1) make them inappropriate for industrial-scale applications. In the same way, the CoCl_2 , which was used by Beller's research team [76], has the lowest price at $792 \text{ } \$/\text{kg}$, needing only $\sim 2 \text{ } \$/\text{kg}$ of H_2 . Notice,

however, that the high price of Bis(2-(diphenylphosphino)ethyl)amine ligand, contributes to the very high total cost.

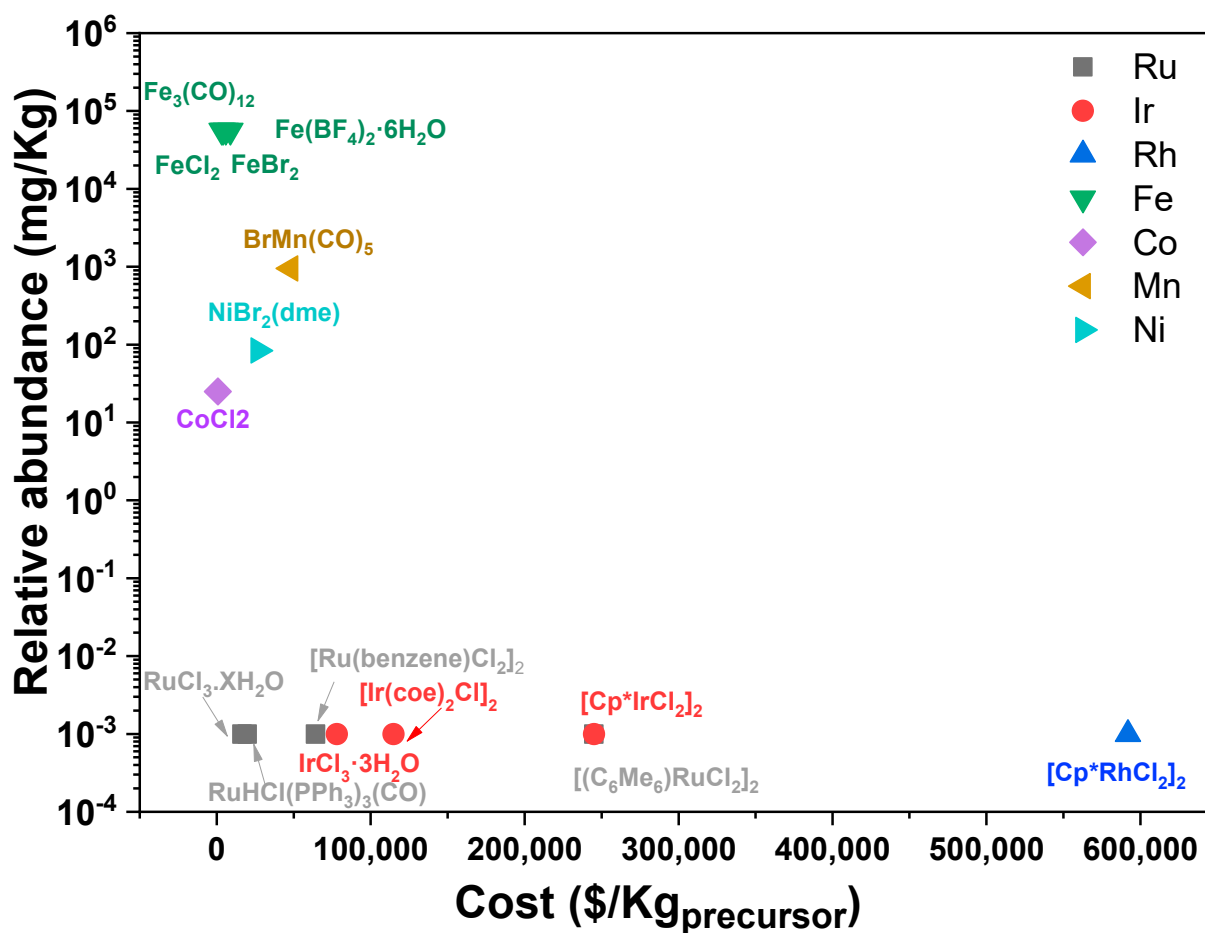


Figure 9. Correlation plot of relative abundance (mg/kg) versus cost (\$/kg) of various metal precursors.

Table 1. Cost analysis based on the metal precursor.

Entry	Metal Precursor	Conditions	TONs	Cost (\$/kg _{metal precursor})	kgH ₂ /kg _{metal precursor}	¹ \$/kgH ₂ (Metal Precursor)	Ref.
#11	RuHCl(PPh ₃) ₃ (CO)	1.42 μmol of catalyst, 35 mL DMF and NH ₃ (33.5 mmol base), T = 90 °C	706,500	19,920	1485	1.34	[51]
#12	[(C ₆ Me ₆)RuCl ₂] ₂	1 μmol catalyst (100 mL, 1 mmol) 2 M aqueous FA solution (10 mL), T = 60 °C	264	245,034	0.79	31,004	[55]
#9	[RuCl ₂ (benzene)] ₂	9.55 μmol of catalyst (19.1 μmol [Ru]), 115 μmol dppe (Ru/dppe = 1:6), 20 mL DMOA T = 90 °C	1,000,000	64,200	4001	1.60	[77]
#13	RuCl ₃ .XH ₂ O	5.95 μmol of Ru, Ru/PPh ₃ = 1/3, 5.0 mL, 5HCO ₂ H/2NEt ₃ , DMF = 1 mL, T = 40 °C	700 (after 3 h)	16,500	6.75	244	[77]

Table 1. Cont.

Entry	Metal Precursor	Conditions	TONs	Cost (\$/kg _{metal precursor})	kgH ₂ /kg _{metal precursor}	¹ \$/kgH ₂ (Metal Precursor)	Ref.
#14	[Ir(coe) ₂ Cl] ₂	1 μmol of catalyst, tri-ethylammonium formate = 5 mmol, tBuOH = 1 mL, THF = 0.1 mL, T = 80 °C	2000	114,828	4.5	2570	[78]
#5	[Cp*IrCl ₂] ₂	1 μmol of catalyst, FA = 5 M, 10.0 mL, T = 90 °C	2,400,000	245,108	34,761	4.07	[44]
#15	IrCl ₃ ·3H ₂ O	9 mM catalyst, FA = 1250 mM in acetic acid,	>11,000	78,000	62.43	125	[79]
#16	[Cp*RhCl ₂] ₂	1 μmol of catalyst (100 mL, 1 mmol) 2 M aqueous FA solution (10 mL), T = 60 °C	3366	592,000	11	5432	[55]
#3	FeBr ₂	10 μmol of catalyst, 2 mL 1,4 dioxane, 3 g FA, 10.86 mmol NEt ₃ , T = 40 °C	>100,000	5900	928	0.64	[68]
#4	FeCl ₂	FA (110 μL, 2.91 mmol), LiBF ₄ = 0.291 mmol, 10 mol%, 5 mL dioxane, T = 80 °C.	983,642	3279	4089	0.08	[71]
#17	[Fe(BF ₄) ₂]·6H ₂ O	Fe(BF ₄) ₂ ·6H ₂ O = 74 μmol, PP ₃ = 296 μmol, 2 mL FA, 50 mL PC, T = 80° C	92,417	4176	68.94	0.76	[70]
#18	Fe ₃ (CO) ₁₂	20 μmol Fe ₃ (CO) ₁₂ /PPh ₃ /tpy (Fe/PPh ₃ /tpy 1:1:1), 5FA·2NEt ₃ = 5 mL, 1 mL DMF, T = 60 °C, 300 W xenon lamp (385 nm cutoff)	126	8903	0.50	1778	[69]
#19	CoCl ₂	10 μmol of catalyst, FA = 50 mmol, HCOOK = 50 mmol, H ₂ O = 18.1 mL, NaBEt ₃ H = 1.5 mL, T = 80 °C	2260	792	35	2.27	[76]
#20	BrMn(CO) ₅	2 mM (10 μmol) of catalyst, 870 mM FA, 5 mL 1,4 dioxane, T = 65 °C	190	45,000	1.38	3254	[72]
#21	NiBr ₂ (dme)	5.3 μmol [Ni], FA/nOctNMe ₂ = 11:10, 5 mL, PC = 5.0 mL, T = 80 °C	626	27,000	4.06	665	[74]

¹ the cost estimation is compiled by introducing a “scale-factor” that can divide the cost on the order of 10.

3.2. Ligands of Catalysts in FA Dehydrogenation

The reactivity of a metal-complex catalyst relies not only on the nature of its metal ion, but also on the ligand(s) which determine its coordination environment, stereoselectivity, charge, and redox properties. Thus, the ligand provides metal-specific electronic and

steric properties, determining in this way its reactivity and modulating metal-substrate interactions during catalysis [80]. Moreover, in hydride chemistry, it is the electron density offered by the ligand that controls the metal oxidation state [81]. Operationally, ligands coordinated to the metal center of homogenous catalysts for FA dehydrogenation could be categorized into three main types [82,83]: (i) phosphine, (ii) N-donor bidentate, and (iii) pincer-type ligands, based on the atoms/groups which act as σ -electron donors and/or π -electron acceptors.

Up-to-date, *phenyl phosphines* are the ligands of choice since they are able to tune the electronic properties of metal via their strong σ -donation capacity/ π -acceptor ability [80], and the increased basicity that in some cases triggers the catalytic reaction (Figure 10). The impact of various phosphine ligands on catalytic H_2 generation utilizing Ru precursors was initially described in 2008 by Beller and coworkers [84]. In the absence of ligands, $RuCl_3 \cdot xH_2O$ was inactive, while $[RuCl_2(p\text{-cymene})]$ and $[RuCl_2(benzene)_2]$ complexes were thought to be the pertinent precursors. Moreover, the addition of triphenylphosphine (PPh_3) accelerated the reaction. Investigating the ratio (Ru precursor:phosphine), it was found that 20 equivalents of PPh_3 maintained the system's activity for more than 6 h. Among the evaluated monodentate and bidentate ligands, PPh_3 and 1,2-bis(diphenylphosphino)butane (dppe) demonstrated the best results [84]. The selective dehydrogenation of FA, under mild conditions, using a non-noble metal, was first reported by Beller et al., in 2010, using an $Fe_3(CO)_{12}$, 2,2',6',2'-terpyridine or 1,10-phenanthroline precursor with the PPh_3 ligand in the presence of light. Although the breakthrough in the field of non-noble metal catalysts, the activity was quite low ($TON \sim 100$, $TOF \sim 200 \text{ h}^{-1}$) [69]. A highly-active non-noble metal catalyst was published by the same group, mixing in situ an $Fe(BF_4)_2 \cdot 6H_2O$ metal precursor with the $[P(CH_2CH_2PPh_2)_3]$ ligand in propylene carbonate as a solvent with $TON > 92,000$ and $TOF = 9425 \text{ h}^{-1}$ [70]. The substitution of phenyl-phosphines with more basic ligands such as nonaromatic cycloalkyl groups resulted in systems not as active as anticipated, because of steric effects [85]. The low solubility of phenylphosphines imposes the use of organic solvents in catalytic FA dehydrogenation. Consequently, ligand solubility affects the behavior of the catalytic system. For example, the addition of hydrophilic moieties to the ligands, such as sulfonate groups, may increase their solubility in water, while broadening the applicability of the phosphine and, in general, catalysts. Within this context, Laurentzy et al., in 2008, were the first group to synthesize water-soluble oligocationic ligands with sulfonate groups [86]. After six years, the same research group investigated different types of (Ru/sulfonated phosphines), further confirming the positive effect of the σ -donating capacity of these phosphine ligands [87].

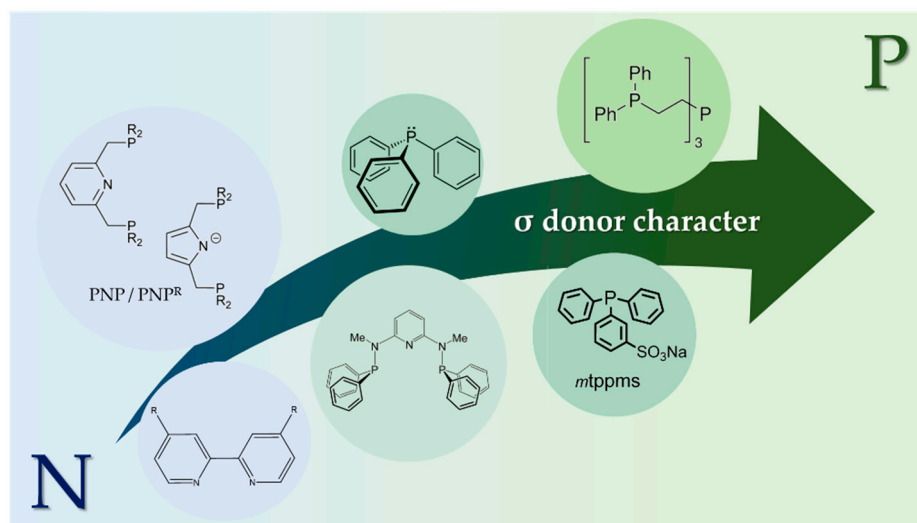


Figure 10. The increasing of σ -donor character proceeding from Nitrogen to Phosphorous compounds.

Bidentate N-donors: The majority of *N-donor* bidentate (Figure 11) metal catalysts include mainly ‘half sandwich-type ligands’ with a Cp*(pentamethylcyclopentadienyl anion) functionality as an electron-donating group which was found to be supported very often by *N-donor bases* to form effective metal catalysts. Their implementation in the field of FA dehydrogenation was initiated in 2008 by the research group of Fukuzumi [88] with the water-soluble $[\text{Cp}^*\text{Rh}(\text{H}_2\text{O})(\text{BPY})]^{2+}$ complex, (BPY = bipyridine). Many of these catalysts are very active in aqueous FA dehydrogenation and exhibit TOF values $> 10,000 \text{ h}^{-1}$ at mild (100°C) conditions [55,56,73]. The modification of N-/N bidentate ligands has been deployed by Himeda et al. in a $[(\text{C}_n\text{Me}_n)\text{M}(4,4\text{-R}_2\text{-BPY})\text{Cl}]^+$ complex, using different R groups (R = Me, OMe, and OH, with metals M = Ru, Rh, Ir/0 [55]. With R = OH), the overall ligand behavior became pH-dependent. Thus, in more basic conditions, the OH group was deprotonated resulting in pH-switchable ligands. The enhanced performance of the catalysts was attributed to the OH groups’ acid–base balance. Moreover, due to the acid–base equilibrium of the ligands, the reaction rate was also impacted by the pH value of the $\text{HCOOH}/\text{HCOONa}$ solution, providing a reversible conversion of H_2/CO_2 to FA, just by changing the pH value [55]. Since the influence of *N,N-donor ligands* was found to be important, further investigations included imidazoline, imidazole, and pyrazole derivatives [73]. The combination of BPY with OH groups and azole ligands contributed to the highly-efficient dehydrogenation of FA [89]. A group of bioinspired, N-based Ir catalysts with pyrimidine-azolin and pyridine-azole ligands was designed by Fujita, Himeda, and their co-workers [57]. They showed that the improved electron-donating capacity of these ligands was essential for the observed high catalytic reactivity. Beyond the finding of optimal electronic properties and the appropriate basicity of the metal center in catalysis, inadequate stability continues to be a significant hurdle to the practical implementation of these catalysts.

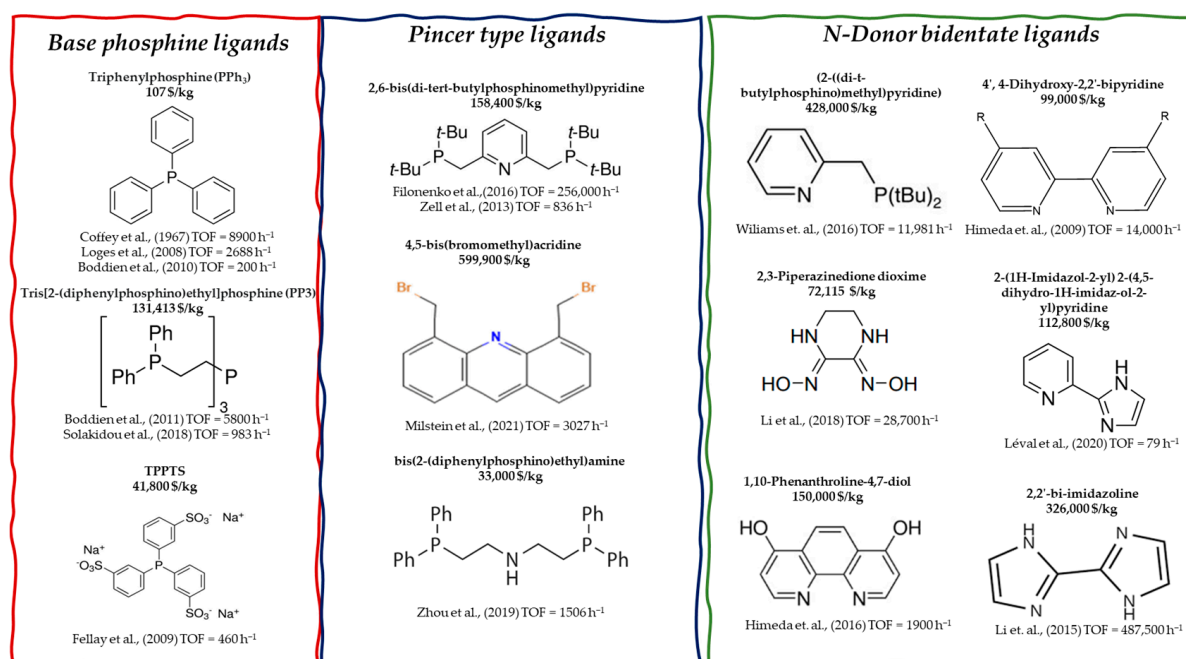


Figure 11. Chemical structure of selected ligands used in cost analysis, from various catalytic systems.

Pincer-type (PNP) Ligands: The design of ligands for pincer complexes (Figure 11) provides a variety of options and possible catalytic uses [90]. For instance, the pincer arm may accommodate a variety of heteroatoms and functions. In addition to the chemical stability, the pincer ligand may play an active role in the catalytic cycle by providing an appropriate coordination site for the substrate, weakening specific bonds (H-X bonds), or accepting/donating electrons and protons, while the metal–ligand interaction may be adjusted by the steric/electronic environment [90]. After Shaw synthesized the first family

of PCP compounds in 1976 [83], numerous new compounds having distinct pincer arms have been synthesized due to the stabilization of the tridentate coordination. Among them, there exists an extensive family of carbene pincers [91], POP [92], PNN [93], and PNP [45,94] ligands.

The first research group that investigated the activity of an Ir-PNP in FA dehydrogenation was Nozaki et al. [78]. In 2016, Gonsalvi and Kirchner suggested a series of Fe-PNP complexes containing the 2,6-diaminopyridine scaffold [95]. Using 0.01 mol% of catalyst and NEt_3 as a base, a TOF of 2635 h^{-1} and a TON = 10,000 after 6 h were achieved. Filonenko et al. developed a $[\text{Ru}(\text{PNP}^{\text{tBu}})\text{H}(\text{CO})\text{Cl}]$ catalyst for H_2 storage [51], which was recently integrated into a 25-kW FA-to-power system [30]. Plietker and co-workers [96] described the utilization of a widely available (PNNP)(acetonitrile) Ru^{II} complex for the reversible and efficient reduction of CO_2 in the presence of DBU as a base. At a catalyst dosage of 0.075 mol%, both the reduction and decomposition of the FA adduct were observed. The reaction system exhibited exceptional durability, the storage capacity was unaffected by five charging-discharging cycles, and the generated H_2/CO_2 mixture can be used in traditional fuel cells [96]. The selective dehydrogenation of FA, under mild conditions, using a non-noble metal was first reported in 2013 by the research group of Milstein, which developed a series of Fe pincer complexes, attaining a TON > 100,000, and TOF > 836 h^{-1} , in the presence of NEt_3 , at 40°C [68]. Schneider and Hazari demonstrated in 2014 [71] that a formate Fe-PNP complex, paired with an appropriate Lewis acid co-catalyst, is highly active for FA dehydrogenation. Consequently, using 0.0001%, of catalyst in the presence of 10% LiBF_4 , a TOF of $196,728 \text{ h}^{-1}$ was achieved after 1 h, and a TON > 985,642. Although this is the greatest yet documented TON for non-precious transition metals, the very low concentration of catalyst makes it impossible to be applicable in a fuel cell. The development of other (non-noble metal/pincer)-based catalysts, is of crucial importance and continues until today with several works by the research teams of Boncella [72], Tondreau [97], and Beller [76]. Participation of P atoms, in conjunction with aromatic moieties, e.g., phenyls or imidazole, in the metal catalyst coordination environment seems to be a good strategy for FA dehydrogenation. Thus, the phosphine-type ligands or PNP pincer ones are widely used [45,95]. When the ligand framework additionally offers π -electron acceptor orbitals from, e.g., double bonds including O- or N-atoms, this very often assists the catalysis [53].

The orientation and the coordination of $\text{HCOOH}/\text{HCOO}^-$ to metal is a crucial parameter also because it tunes the catalyst's environment towards formation of metal-hydride species via β -H elimination from $\text{HCOOH}/\text{HCOO}^-$, which is probably the rate determinant step in FA dehydrogenation [98]. To improve long-term stability, a Ru/tetraphos-1 P4 catalyst [99] was used. In the presence of an amine additive, the system was active for FADH under both batch and continuous-feed conditions. Using NMR tests and DFT simulations, the authors analyzed the reaction process. It was shown that a *trans*- $[\text{Ru}(\text{H})_2(\text{meso-P}_4)]$ is the critical intermediate in the postulated catalytic cycle, indicating that FA activation occurs on just one of the hydrides of the octahedral species. In addition, the created gas mixtures were directly fed to a typical PEM fuel cell for producing electric power. Continuing the investigation of Fe-pincer complexes, Gonsalvi et al. tested Fe-tetraphos-1, P4, complexes, for the additive-free selective FA dehydrogenation at 60°C with TONs > 6061 and TOF = 1570 h^{-1} [100]. As a significant drawback, batch recycling experiments revealed a significant decline in activity from the 1st to the 3rd cycle, suggesting deactivation of the catalyst.

Comparing the cost of the three categories of ligands (N,N bidentate, Pincer, Phosphine), it seems that the most expensive is the pincer-type ligand category with a price range between 599,000 \$/kg for 4,5-bis(bromomethyl)acridine and 33,000 \$/kg for Bis[(2-diisopropylphosphino)ethyl]amine. The high performance ($9326 \text{ kg H}_2/\text{kg}_{\text{ligand}}$) can balance the cost of Entry #2, (see Table 2) with 6.43 \$/kg H_2 . Although Entry #6b has lower TONs, the cheaper Bis[(2-diisopropylphosphino)ethyl]amine has a value score of 0.81 \$/kg H_2 . 2,6-Bis(di-tert-butylphosphino)pyridine, which was used in several

PNP-complexes for FA dehydrogenation [51,68,101], has a price of 158,000 \$/kg with the example of Entry #1 presenting low price ~2.85 \$/kg H₂. The triphos ligand has a relatively low cost of 39,200 \$/kg_{ligand}, albeit with a modest catalytic efficiency (32 kg H₂/kg_{ligand}), which contributes to the relatively high value of 122 \$/kg H₂.

The high-performance N,N-bidentate ligands present a lower price, with 150,000 \$/kg_{ligand} for 4,7-Dihydroxy-1,10-phenanthroline and 600 \$/kg for 2,2-Bipyridine. The very low \$/kg H₂ term, (0.32 \$/kg H₂) makes the use of this ligand appropriate for mobile applications, despite the high price. Within this context, Léval et al. [73] tested various ligands with a N–H moiety, i.e., pyrazole or imidazole (Entry #26, #26a) and bipyridine (Entry #26b) with a Mn(CO)₅Br metal precursor. Bipyridine showed a very low performance with 0.64 kg H₂/kg_{ligand}, in contrast with 2-(4,5-dihydro-1H-imidazol-2-yl)pyridine and 1H,1'H-2,2'-Biimidazole which presented a higher efficiency with 7.82 kg H₂/kg_{ligand} and 3.26 kg H₂/kg_{ligand}, respectively. Despite the high cost of pyrazole and imidazole moieties (112,800 \$/kg_{ligand} and 2840 \$/kg_{ligand}) vs. the cheaper bipyridine (600 \$/kg_{ligand}), the higher efficiency balances the final cost to 7.82 \$/kg H₂ and 3.26 \$/kg H₂ vs. 443 \$/kg H₂. A diaminoglyoxime ligand was recently used by the research group of Li [56], introducing a new family of N,N-bidentate ligands in the field of FA dehydrogenation. Its relatively low price (72,115 \$/kg_{ligand}) in tandem with high performance (12,610 kg H₂/kg_{ligand}) leads to a very low cost of 0.76 \$/kg H₂.

The widely used phosphine ligands are the cheapest with moderate catalytic activity. In most cases, they are commercially available and mixed in situ with metal precursors. Examples include the work of Beller [47,49] and Laurentzy [50,86] who tested various phosphines, with the cheapest but less effective being the PPh₃ (107 \$/kg_{ligand}) [69,77,79]. The more expensive, water-soluble TPPTS with 41,800 \$/kg_{ligand}, gives a Ru-TPPTS complex costing 59 \$/kg H₂, while a more efficient Ir catalyst achieves a five times lower price (11.8 \$/kg H₂). Tetradentate phosphine PP₃, although it contributes to a more stable and higher-performing system [53,70], is far more expensive than the monodentate analogue PPh₃ (131,413 \$/kg_{ligand} vs. 107 \$/kg_{ligand}). The low-performance Fe₃(CO)₁₂/PPh₃ complex has a cost of 11 \$/kg H₂, [69] while the stable and long-term activity of [Fe(BF₄)₂·6H₂O]/2PP₃ catalyst cannot compensate for the PP₃ ligand cost, having a 15-fold higher price at ~191 \$/kg H₂ [70].

Table 2. Cost analysis based on the ligand.

Entry	Ligand	Conditions	TONs	Cost (\$/kg _{ligand})	kgH ₂ /kg _{ligand}	¹ \$/kgH ₂ (Ligand)	Ref.
#1	tBu-PNP (2,6-Bis(di-tert-butylphosphinomethyl)pyridine)	1.0 µmol of catalyst FA = 0.3 mL/h, NEt ₃ = 1.50 mL, 0.7 mL DMSO, T = 90 °C	1,100,000	158,400	5565	2.85	[101]
#2	4,5-bis(bromomethyl)acridine	40 µmol (23 mg) catalyst, FA = 5 mL, (0.13 mol), T = 95 °C	1,701,150	599,900	9326	6.43	[102]
#22	1,1,1-tris-(diphenylphosphinomethyl)ethane (triphos)	12.9 µmol catalyst, 12.9 mmol FA FA:OctNMe ₂ = 11:10 = (2.73 mL), T = 80 °C	10,000 (after 6 h)	39,200	32	122	[103]
#13	PPh ₃	5.95 µmol of Ru, Ru/PPh ₃ = 1/3, 5 HCO ₂ H/2NEt ₃ = 5 mL, DMF = 1 mL, T = 40 °C	700	107	1.78	6.00	[77]
#9	dppe	9.55 µmol [RuCl ₂ (benzene)] ₂ (19.1 µmol [Ru]), 115 µmol dppe (Ru/dppe = 1:6), FA added continuously, 20 mL DMOA, T = 60 °C	1,000,000	2760	834	0.33	[49]

Table 2. Cont.

Entry	Ligand	Conditions	TONs	Cost (\$/kg _{ligand})	kgH ₂ /kg _{ligand}	¹ \$/kgH ₂ (Ligand)	Ref.
#23	TPPTS	[Ru(H ₂ O) ₆](tos) ₂ = 1.5 mmol, TPPTS = 3 mmol, FA added continuously, 12 mL FA/HCOONa (4 M, 9:1), T = 100 °C Aqueous catalyst stock solution = 0.2 mL, 1.0 µmol final concentration, FA = 10.0 M, 220 mL, T = 70 °C	40,000	41,800	5281	59.36	[50]
#7	2,3-Piperazinedione dioxime	1 µmol of catalyst, FA = 40 vol%, 10 mol L ⁻¹ , 22 MPa, T = 80 °C	5,200,000	72,115	12,610	0.76	[56]
#6	4,7-Dihydroxy-1,10-phenanthroline	1 µmol catalyst (100 mL, 1 mmol), 2 M aqueous FA solution = 10 mL, T = 60 °C	5,000,000	150,000	47,154	0.32	[65]
#24	4',4'-Dihydroxy-2,2'-bipyridine	9.8 µmol catalyst, FA = 133 mmol/catalytic cycle HCOONa = 50 mmol, V _{total} = 20.0 mL, T = 100 °C	18,667	99,000	199	49.9	[55]
#25	mtpms	20 µmol Fe ₃ (CO) ₁₂ /PPh ₃ /tpy (Fe/PPh ₃ /tpy = 1:1:1), 5FA·2NEt ₃ = 5 mL, 1 mL DMF, 300 W xenon (385 nm cutoff), T = 60 °C	>67,650	41,800	371	11.28	[104]
#18	PPh ₃	Fe(BF ₄) ₂ ·6H ₂ O = 74 µmol, PP ₃ = 296 µmol, 2 mL FA, 50 mL PC, T = 80 °C	126	107	0.96	11.13	[69]
#17	PP ₃	0.001 mol% [Fe], FA = 110 µL, (2.91 mmol), LiBF ₄ = 0.291 mmol, 10 mol%, 5 mL 1,4 dioxane, T = 80 °C	92,417	131,413	68.94	191	[70]
#4	Bis[(2-diisopropylphosphino)ethyl]amine	0.005 mmol catalyst, FA = 37 mmol, HCOOK = 40 mmol, H ₂ O = 9 mL, triglyme = 4 mL, T = 92.5 °C	983,642	33,000	4089	0.81	[71]
#26	2-(4,5-dihydro-1H-imidazol-2-yl)pyridine	0.005 mmol catalyst, FA = 37 mmol, HCOOK = 40 mmol, H ₂ O = 9 mL, triglyme = 4 mL, T = 92.5 °C	564 (after 3 h)	112,800	7.67	7.82	[73]
#26a	2,2-Bipyridine	0.005 mmol of catalyst, FA = 37 mmol, HCOOK = 40 mmol, H ₂ O = 9 mL, triglyme = 4 mL, T = 92.5 °C	50 (after 3 h)	600	0.64	443	[73]
#26b	1H,1'H-2,2'-Biimidazole	HCOOK = 40 mmol, H ₂ O = 9 mL, triglyme = 4 mL, T = 92.5 °C	220 (after 3 h)	2840	3.28	3.26	[73]

¹ the cost estimation is compiled by introducing a “scale-factor” that can divide the cost on the order of 10.

3.3. Additives/Cocatalysts in FA Dehydrogenation

Many systems in FA dehydrogenation employ the use of additives or cocatalysts, (Figure 12), either as an essential component for the operation of the system or to improve the total performance of the system. As we have outlined recently [98], additives and catalysts should be distinguished in terms of function: *Additives* are sacrificial agents that typically are consumed stoichiometrically with the HCOOH atoms. On the other hand, *co-catalysts* are used at very low concentrations, i.e., typically close to that of the catalyst itself. Thus, in terms of price analysis, cocatalysts are by far preferable.

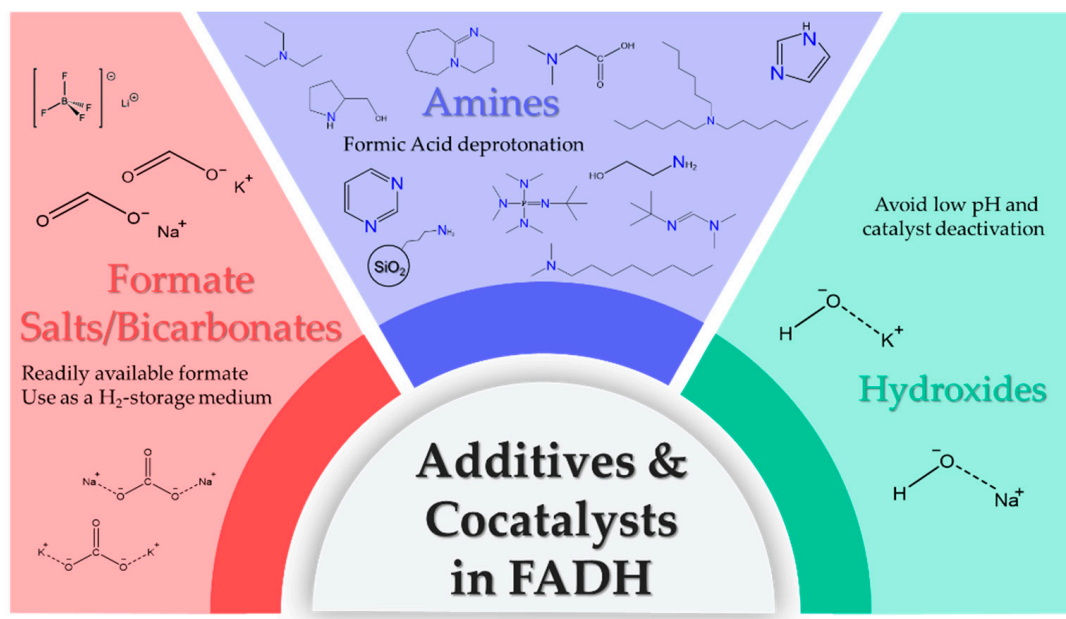


Figure 12. Some additives and cocatalysts utilized in FA dehydrogenation.

The kind of additive or cocatalyst (amine, Lewis acid, etc.) depends on the mechanistic aspects in which it is to be involved. The choice for a specific substance as eligible for additive or cocatalyst is determined by several factors, such as polarity [105], volatility [106], flammability [107], toxicity, solvent miscibility [47], and in general easy handling and compatibility with the existent system. Moreover, a future application of a system in a fuel cell setup dictates some operational and cost-related limitations.

The use of amines and hydroxides, (Figure 12) has been widely implemented as additives for the FA dehydrogenation to avoid a low pH of the reaction solution, which presumably could deactivate the catalyst [102]. Moreover, amines have been utilized as additives due to their ability to activate the catalyst precursor via FA deprotonation. The amines' activity increased with increasing their carbon chain length [77]. On the other hand, low gravimetric and volumetric H₂ densities, which represent one of the drawbacks of FA as an energy carrier, are further affected by the presence of additives. Moreover, the volatility of amines (e.g., NEt₃) poses a serious drawback in their use, since they may contaminate the gaseous products in a continuous H₂ generation process, which would necessitate gas purification before their utilization in a fuel cell [108]. The problem of amine volatility is intensified in most cases due to the high temperatures at which most systems operate [109]. To avoid this problem, the application of less volatile amines (e.g., HexNMe₂) has been already suggested [49,84], or in place of amines, the use of amino-functionalized SiO₂ nanoparticles in the heterogeneous phase. Our research group has demonstrated that the heterogenized amino H₂N@SiO₂ functionalities (97 μmol of NH₂-groups over 52 mmol of FA) with a homogeneous [Ru/PP₃/FA] system may increase H₂-production by six times compared to liquid n-propylamine in the same amount [110]. Moreover, the heterogenized co-catalyst H₂N@SiO₂ may be reused four times with a 5% activity loss after each usage. Bielinski et al. [71] presented a homogeneous Fe catalyst that when utilized in conjunction

with a Lewis acid (LA) co-catalyst achieved TON~1,000,000 for FA dehydrogenation. They evaluated many LAs, with LiBF_4 being the most effective. Preliminary studies indicate that LA aids in the decarboxylation of a crucial Fe-formate intermediate and can also be employed to boost the CO_2 hydrogenation process in reverse [71].

H₂O-solvent/pH-Effect. Another feature of molecular catalysts which are active in aqueous solutions and should always be taken into account is pH dependence. Specifically, pH conditions determine the H_2 production rate by gating the rate-limiting protonation/deprotonation events. Hydroxides, such as NaOH, in most studies are used for modulating the pH value. A typical case is the Ru-Ir heterometallic complex $[\text{Ir}^{\text{III}}(\text{Cp}^*)(\text{H}_2\text{O})(\text{bpm})\text{Ru}^{\text{II}}(\text{bpy})_2](\text{SO}_4)_2$ in water showing a characteristic pH-dependence of TOFs, attaining the highest TOF of 450 h^{-1} at $\text{pH} = 3.8$ which coincides with the pK_a of FA deprotonation. In general, maximum efficiency is observed at moderately acidic pH values in the region of 4–6, where FA deprotonation is promoted and thus the formate anion is available to be inserted in the catalytic cycle [111]. In this context, Léval et al. [73] demonstrated that an imidazoline-based ligand was effective for manganese-catalyzed FADH in H_2O /triglyme solution containing KOH. It was discovered that the performance of the Mn-2 catalyst decreased when the pH rose caused by the consumption of FA. Therefore, the catalytic performance might be maintained through the use of a pH buffer. A Mn-containing pyridyl-imidazoline ligand converted FA to 14 L of H_2/CO_2 mixed gases (TON 5736) and was stable for over three days [73]. As a final point, catalytic systems based on molecular complexes that exhibit sensitivity in water (as solvent or traces) usually require special treatment, i.e., purification of all the reagents and components, extra sacrificial agents, and expensive solvents for high efficiency or pH adjustment, and further increase the total budget for the FA dehydrogenation process.

Formate salts vs. Formic acid as H₂-Source. Formate salts are non-acidic, and therefore catalyst stability is of lesser concern [102,112]. In addition, they are non-volatile and non-toxic [106,112] and can contribute as an H_2 -source medium. Another beneficial aspect of storage of H_2 in the form of solid formate salts is the approach is geographically independent with no requirement for proximity to a salt stock. The term ‘potential H_2 density’, signifies the amount of H_2 that can be released from a kilogram of formate-salt when it is dissolved in aqueous media. As an example, for sodium formate (HCOONa), the potential density is ca. 28 g H_2 /L of a saturate solution of HCOONa [112], while between the range of 20 and 80 °C, HCOOK shows the highest volumetric H_2 storage capacity [112]. However, the usable H_2 density is limited by the solubility of the corresponding bicarbonate salt due to CO_2 formation during catalysis [112]. This in turn depends on the cation (e.g., Na^+ , K^+) [113] and the reaction temperature. For example, potassium formate (HCOOK) shows the highest solubility, ca. 14 M, in aqueous media at room temperature, and provides a theoretical H_2 capacity of 29 g H_2 /L [112]. Due to this correlation, formate salts have been incorporated in reversible H_2 storage systems based on a CO_2 (HCO_3^-)/ H_2 and formate equilibrium [20,107]. This has been reported for the $\text{HCOONa}/\text{Na}_2\text{CO}_3$ [107] and the $\text{HCOOK}/\text{KHCO}_3$ system [31].

The most commonly used additive type is the amines. Triethylamine (NEt_3) $\geq 99.5\%$ has a cost of 235 \$/kg on a lab scale, while in industrial quantities can be supplied at the price of approximately \$63 per kg, (Figure 13), being one of the simplest and low-cost amines that have been utilized in many FADH systems with both noble and non-noble metals (Table 3) [68,101]. The analogue amine NBU_3 , in addition to the higher price (106 \$/kg on an industrial scale), has an efficiency two times lower (1.08 kg H_2 /kg_{additive}, vs. 1.82 kg H_2 /kg_{additive}), gauging the final price at 9.78 \$/kg H_2 vs. 3.46 \$/kg H_2 . However, due to its volatility, NEt_3 has been replaced in other systems by bulkier yet costlier molecules, such as $n\text{OctNMe}_2$ [99] (\$200 per kg), NHex_3 [51] (\$154 per kg), or Me_2NDec (84\$ per kg) [49] (industrial-scale cost). Lab-scale vendors offer $n\text{OctNMe}_2$, NHex_3 and Me_2NDec at the cost of 3399 \$/kg, 1493 \$/kg, and 2388 \$/kg, respectively. Although Me_2NHex contributes to the highest catalytic performance with 2.68 kg H_2 /kg_{additive} [49], it is used less due to its

high price (\$ 6119 per kg) in terms of lab-scale cost, while on an industrial scale its price can drop only two times, i.e., 3166 \$/kg.

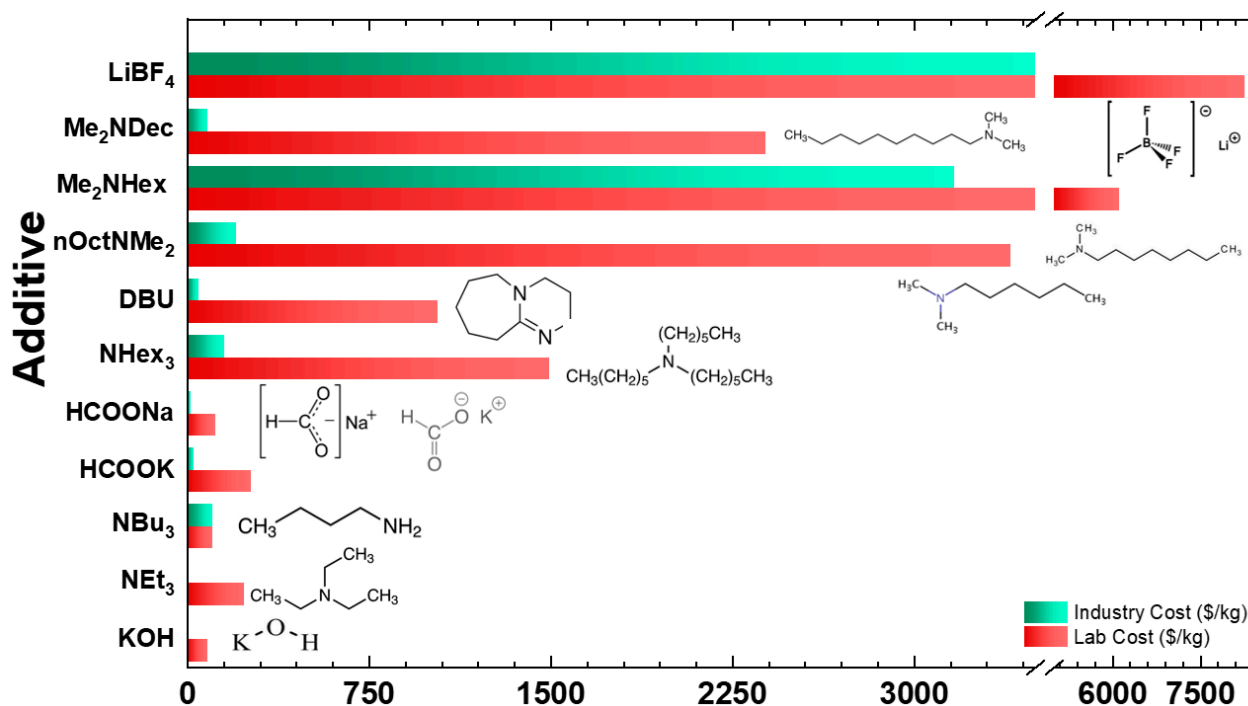


Figure 13. Lab-scale vs. industrial-scale cost of selected additives used for FA dehydrogenation.

Table 3. Cost analysis based on the additive.

Entry	Additive	Conditions	TONs	Cost (\$/kg _{additive})	kgH ₂ /kg _{additive}	² \$/kgH ₂ (additive)	Ref.
#3a	NBu ₃	21.8 μmol catalyst, FA = 1 g, 10.86 mmol NBu ₃ , 2 mL THF, T = 40 °C	¹ 50,000	106	1.08	9.78	[68]
#3	Net ₃	10 μmol catalyst, FA = 3 g, 10.86 mmol NEt ₃ , 2 mL 1,4 dioxane T = 40 °C	100,000	63	1.82	3.46	[68]
#9	nOctNMe ₂	9.55 μmol [RuCl ₂ (benzene)] ₂ (19.1 μmol [Ru]), 115 μmol dppe (Ru/dppe = 1:6), 20 mL nOctNMe ₂ , T = 60 °C	1,000,000	200	2.5	8	[49]
#9a	Me ₂ NHex	9.55 μmol [RuCl ₂ (benzene)] ₂ (19.1 μmol [Ru]), 115 μmol dppe (Ru/dppe = 1:6), 20 mL Me ₂ NHex, T = 60 °C	¹ 1,041,355	3166	2.68	116	[49]
#9b	NHex ₃	9.55 μmol [RuCl ₂ (benzene)] ₂ (19.1 μmol [Ru]), 115 μmol dppe (Ru/dppe = 1:6), 20 mL NHex ₃ , T = 60 °C	¹ 378,675	154	0.95	16.3	[49]
#9c	Me ₂ NDec	9.55 μmol [RuCl ₂ (benzene)] ₂ (19.1 μmol [Ru]), 115 μmol dppe (Ru/dppe = 1:6), 20 mL Me ₂ NDec	¹ 358,744	84	0.88	9.53	[49]
#11	NHex ₃	1.42 μmol of catalyst, continuous flow of FA, NHex ₃ = 33.5 mmol, 35 mL DMF, T = 90 °C	706,500	154	0.21	73.39	[51]
#9d	DBU	1.42 μmol of catalyst, continuous flow of FA, DBU = 33.5 mmol, 35 mL DMF, T = 90 °C	310,000	46	0.16	28.2	[51]
#9e	Net ₃	1.42 μmol of catalyst, continuous flow of FA, Net ₃ = 33.5 mmol, 35 mL DMF, T = 90 °C	326,000	63	0.26	24.37	[51]

Table 3. Cont.

Entry	Additive	Conditions	TONs	Cost (\$/kg _{additive})	kgH ₂ /kg _{additive}	² \$/kgH ₂ (additive)	Ref.
#4	LiBF ₄	0.001 mol% [Fe], FA = 110 µL, (2.91 mmol), LiBF ₄ = 0.291 mmol, 10 mol%, 5 mL 1,4 dioxane, T = 80 °C 9.8 µmol catalyst,	983,642	3760	7215	0.05	[71]
#25	HCOONa	FA = 133 mmol/catalytic cycle HCOONa = 50 mmol, V _{total} = 20.0 mL, T = 100 °C	>67,650	14	0.39	3.6	[104]
#26c	HCOOK	0.005 mmol catalyst, FA = 37 mmol, HCOOK = 40 mmol, H ₂ O = 9 mL, triglyme = 4 mL, T = 92.5 °C	5746 (after 45 h)	27	0.21	12.6	[73]
#26d	KOH	0.37 mmol of catalyst, FA = 5 mmol, KOH = 40 mmol, H ₂ O = 9 mL, triglyme = 4 mL, T = 92.5 °C	2895	120	1.42	8.4	[73]

¹ the TONs are calculated approximately for continuous operation, using those additives. ² the cost estimation is compiled by introducing a “scale-factor” that can divide the cost on the order of 10.

The cost of using formate salts, is low compared to other additives, with HCOONa being the cheapest (\$14 per kg), while HCOOK is costlier at \$27 per kg. At lab-scale cost, the prices are 10 times higher with 116 \$/kg and 264 \$/kg, respectively. Among hydroxides, KOH (120 \$/kg) is the most frequently used, modulating the pH value of various systems [54,73,111] or replacing the formate salts. Interestingly, in a Mn(pyridine-imidazoline)(CO)₃Br catalytic system the addition of KOH instead of HCOOK could produce 1.42 kg H₂/kg_{additive} with a cost of 8.4 \$/kg H₂ [73]. Lewis acid (LA) co-catalyst, LiBF₄, despite its high price (3760 per kg), exhibits very high performance, resulting in a cost of 0.05 \$/kg H₂ [71].

3.4. Solvent Media in FA Dehydrogenation

Another key parameter that affects the overall performance and feasibility of H₂ production systems and contributes to the total cost of the catalytic system is the solvent. The nature of a solvent in catalytic FA dehydrogenation has been proven essential for the majority of the currently reported efficient homogeneous molecular catalysts [114] and a considerable number of used organic solvents have been described in the literature. The dielectric constant of the solvent, its volatility, polarity, and its protic or aprotic characteristics vastly determine the catalytic mechanism, especially in systems where outer-sphere interactions between the ligands and water, when acting as a solvent, govern the protonation of a hydride species [44,115,116]. Some of the most used polar aprotic solvents include propylene carbonate (PC), dimethyl carbonate (DMC), chlorobenzene, tetrahydrofuran (THF), dimethylformamide (DMF), and dimethyl sulfoxide (DMSO), while dioxane, benzene, toluene, and dimethoxy ethane (DME) are widely selected as non-polar aprotic solvents for FA dehydrogenation. Polar protic solvents, such as methanol, ethanol, tert-butanol, and water, are more likely to take part in deprotonation events [98]. In some cases, the use of solvent mixtures with different polarities can enhance the catalyst's activity by lowering the barrier of the turnover-limiting step of the catalytic mechanism. Generally, the selected solvent usually affects the change in entropy and enthalpy via the solvation process for both the reactants and products [117].

Solvent selection in FA dehydrogenation can be attributed to some substantial advantages to the system [59], e.g., (a) solubility of the catalytic complex and/or cocatalyst, (b) stabilization of the intermediate active species, facilitating the coordination to the metal center, or (c) decrease of activation energy barrier. Moreover, considering the fact that some basic additives are also used as solvents (e.g., Net₃, DMOA), they can contribute to the low acidity of the reaction solution since low pH values, arising from FA, have been reported to lead to catalyst deactivation via irreversible formation of inactive species [118].

Additionally, some studies indicate that the solvent has a slight effect on the activation energy of the catalytic system [70]. Nevertheless, taking into consideration that small activation energy barriers are highly desirable in catalytic procedures to allow lower operating temperatures [98], and thus less total energy consumption, the choice of solvent should be made wisely. Despite the aspects of using a solvent, from a mechanistic point of view, lately, scientific research has focused on FA dehydrogenation under solventless conditions. A major drawback of using solvents is the fact that the maximum gravimetric and volumetric H₂ density is not fully exploited and thus the total energy density of the whole catalytic system is limited [70,119]. Another downside related to practical issues is the high volatility of the most used solvents, which leads to vapor generation in the gas mixture and consecutively in fuel cell destruction (the same as additives). Moving towards the direction of full H₂ storage capacity of FA, recently, Kar et al. [102] reported excellent catalytic activity of a ruthenium 9H-acridine pincer complex for FA dehydrogenation. The catalyst exhibited stability in neat FA even at high temperatures and reached TONs of 1,701,150 within a month and TOF as high as 3067 h^{−1}. This is a promising sign that the H₂ economy is a viable solution to the global energy crisis as the absence of solvents and additives drastically minimizes the expenditures of the process. Moreover, considering the fact that the use of environmentally friendly procedures is extremely desirable in order to meet the universal standards for practical implementations, the available environmentally benign solvents are scarce. In large-scale H₂ production, the use of huge amounts of solvents, i.e., liters or tons, not only increases the final cost of the procedure, but also intensifies the possibility of them being discharged into water sources and results in further contamination of the ecosystem.

The case of water as an alternative cost-efficient solvent: The development of molecular catalysts for FA decomposition that proceed under solventless conditions is still in the early stages and plenty of synthetic and mechanistic improvements need to be made in order to make these catalytic systems applicable and competitive enough.

On the other hand, a huge number of publications focus on the use of water as a solvent and as an alternative approach towards more environmentally friendly H₂ production systems. Apart from the benign nature of water, its use as a solvent or in solvent mixtures is highly preferable during catalysis as it overcomes problems related to the loss of volatile organic solvents and additives including amines [120]. Considering the applicability of the catalysts for large-scale H₂ production, molecular catalysts that withstand the presence of water are attractive candidates for H₂ production systems that operate on an industrial level, since commercial FA contains water at various amounts depending on its purity level (2–3%) [51,98,102]. In addition, it should be underlined that water is considered an economically advantageous solvent for large-scale implementation of the catalytic hydrogen production procedures, yet its consumption should be made under specified restrictions. By now, huge quantities of water are depleted by a wide range of other processes, namely irrigation and agriculture (65% of the available freshwater), electrolysis, photocatalysis, and other industrial procedures (10% of the total available water). Therefore, a conflict of interest could emerge with respect to the reduced water availability at a global level [121].

The beneficial role of water during FA dehydrogenation using catalytic systems based on the majority of the Ir complexes has been ascertained [102]. An example of a highly efficient catalytic system in water as a solvent without any additives developed by Lu et al. is the iridium complex Cp*Ir bearing diaminoglyoxime ligand that achieved TONs of up to 3,900,000 with an average rate of 65,000 h^{−1} at 90 °C [56]. In some cases, the use of mixtures of water with a second solvent has been proven to enhance the rate of FA dehydrogenation. More specifically, Ikariya et al. stated the improved activity of half-sandwich Ir(III) complexes bearing ligands with a crucial NH functionality in solvent mixtures of water/DME 50:50 (v/v) versus the case where DME is implemented as the sole solvent [122]. The higher performance of the system was attributed to the hydrogen bonding of water onto the acidic amine proton leading to the stabilization of a six-membered transition

state. The metal hydride formation and protonation increase the total H_2 formation rate in conformity with the proton-relay mechanism. Nevertheless, a complete deactivation of the catalyst was observed when only water was used as a solvent, due to poor catalyst solubility, and thus a second solvent is employed in order to alleviate obstacles arising from insolubility [114].

On numerous occasions, low catalyst performance due to insolubility in water or aqueous solutions constitutes one of the main reasons for water being replaced by various aprotic solvents for FA decomposition. Yet, the presence of traces of water in aprotic solvents could hinder, to a lesser extent, the catalytic efficiency. A representative example is a highly active catalyst comprising of $Fe(BF_4)_2 \cdot 6H_2O$ and four equivalents of PP_3 (=tris[2-(diphenylphosphino)ethyl]phosphine) ligand developed by Beller's and Laurency's groups, in PC as a solvent, yielding TOFs of up to $9425\ h^{-1}$ and TONs of over 92,000 at $80\ ^\circ C$ [70]. The investigation of the solvent's effect on the catalyst's activity using several polar solvents revealed that water was inappropriate due to the low catalyst solubility. However, traces of water arising from propylene carbonate did not drastically affect the catalyst's efficiency [123]. Recently, our research group pointed out that a severe catalytic hindrance is observed in this system when water is present in the solution up to 6% [98]. The low catalytic performance of certain molecular catalytic systems in the presence of water or in aqueous solutions has been attributed in individual cases to the competition of the water molecule regarding its coordination to the metal center [56]. This can be entirely understandable when taking into consideration that any atom/molecule coordinating irreversibly to the metal center, apart from the hydride, acts as an inhibitor of the catalytic hydrogen formation [98]. In this context, M. Montandon-Clerc et al. modified the hydrophobic PP_3 compound towards the water-soluble phosphine ligand (PP_3TS) through aromatic sulfonation of its phenyl rings reaching TONs up to 13,000 after 30 recycling experiments, indicating that solubility plays a crucial role for the effectiveness of the FA decomposition [124]. The water-soluble Ir complex bearing an N,N-diimine backbone designed by Wang et al. achieved TOFs of $171,000\ h^{-1}$ with a very high TON of 2,400,000 for FA dehydrogenation in the absence of any additive [44].

Ionic liquids (IL) as solvents for FA dehydrogenation: Since Deng and co-workers reported the use of ionic liquids (ILs) as the reaction media for FA dehydrogenation, much attention has been focused on the role of the ionic liquids as solvents, not only in the field of H_2 production from FA, but also generally in catalysis due to their versatility [106]. Ionic liquids are organic salts (saline compounds) and liquid electrolytes which present exceptional physicochemical properties for catalysis, namely low melting point at room temperature, low vapor pressure, adjustable polarity, solubility, and miscibility, as well as considerably low volatility, which avoids solvent contamination of the produced H_2 stream during the FA dehydrogenation process [124–126]. The strong solvation power and the multiple solvation interactions of the ILs render them a new class of green solvents with various applications in catalysis [127–129]. More specifically, it has been reported that imidazolium ionic liquids act as excellent reaction mediums by facilitating the stabilization of several transition metal catalysts and promoting the catalyst's recycling [129]. In 2010, Yasaka et al. studied the equilibrium for the reversible decomposition of FA into CO_2 and H_2 in the ionic liquid (IL) 1,3-dipropyl-2-methylimidazolium formate [130]. Moreover, the functionalization of ILs solvents with different types of functional groups into the alkyl chains of the imidazolium or pyridinium units has proven to be effective for numerous catalytic processes. An illustrative example is the H_2N -functionalized ILs which have been used to absorb CO_2 [131] and the $(CH_3)_2N$ -functionalized ILs used to promote the hydrogenation of CO_2 to FA [132]. The findings revealed that the equilibrium is strongly favored to the FA side as a consequence of the strong solvation of FA in the IL via the intense Coulombic solute-solvent interactions. On the contrary, when water was used as the solvent without the presence of IL, the solvation process of the FA was weaker. Hence, a 100-fold reduction of the implemented pressure for CO_2 hydrogenation was achieved. As a consequence, H_2 storage using FA could be realized under mild conditions along with a reduction

of the overall cost due to the absence of extremely energy-demanding conditions [130]. Li et al. employed the commercially available IL 1-butyl-3-methylimidazolium chloride (BMimCl) as a solvent for the FA decomposition using the Ru-based catalyst, $[\{\text{RuCl}_2(\text{p-cymene})\}_2]$ with $\text{iPr}_2\text{NEt}/\text{HCOONa}$ as a base and the system produced 725 mL of gas in 2 h ($\text{TON}_{2\text{h}} = 240$). Subsequently, they synthesized several amine-group-functionalized ILs with the $\text{iPr}_2\text{NEMimCl}$ being the most effective IL for the FA dehydrogenation without the addition of any volatile organic amines ($V_{2\text{h}} = 971$ mL, $\text{TON}_{2\text{h}} = 1267$) [106]. In another study, Scholten et al. used the Ru complex $[\{\text{RuCl}_2(\text{p-cymene})\}_2]$ dissolved in the 1-(2-(diethylamino)ethyl)-3-methylimidazolium chloride IL as the solvent without additional bases and the system showed remarkable catalytic activity for the FA decomposition at 80 °C, attaining a TOF of 1540 h^{-1} and excellent recyclability [133]. In addition, Berger et al. [127] reported the highly active and durable catalytic system of RuCl_3 dissolved in the 1-ethyl-2,3-dimethylimidazolium acetate IL as the solvent, obtaining the catalyst ($\text{RuCl}_3/[\text{EMMIM}][\text{OAc}]$). The catalyst reached a TOF of 150 h^{-1} at 80 °C and was able to be recycled over 10 times [127]. The authors stated that the catalyst's performance is dictated by the nature of the IL anion. Moreover, plenty of studies clearly demonstrate that the use of ILs offers the advantage of catalyst isolation and reuse through immobilization techniques [134].

Over and above, considering the practical aspects of the low volatility of the ILs and consequently the non-poisonous effect on the fuel cells along with their lower cost (1.24 \$/kg) compared to other solvents, such as PC (41.15 \$/kg) or 1,4 dioxane (15.78 \$/kg) [135], it is clear that ILs are promising solvents for the FA dehydrogenation in large-scale hydrogen production processes.

Figure 14 depicts the cost variation between the lab-scale and industrial-scale usage of selected solvents for FA dehydrogenation. Specifically, 1,4-dioxane, a toxic and frequently used solvent, costs 154 \$/kg (anhydrous, 99.8%) for lab-scale use while its cost drops to 48 \$/kg for industrial use. This corresponds to an 89% reduction in cost. Propylene carbonate (PC), an environmentally benign solvent with a desirable high boiling point of 242 °C, is estimated to cost around 179 \$/kg (anhydrous, 99.7%) for lab-scale implementation. At the same time, the industrial grade of PC costs 41 \$/kg (99% assay, Alfa Aesar Ltd. Kandel, Germany) while some suppliers provide it at 1.0–1.3\$ per kg (100% assay, Anhui Eapearl Chemical Co., Ltd., Tongling, Anhui Province, China.). Thereby, an entire 87% reduction of the solvent expenses is attained. Tetrahydrofuran (THF), a flammable and carcinogen solvent, listed in the Hazardous Substances List due to its noxiousness, costs around 112.2 \$/kg (Sigma-Aldrich, liquid chromatography grade). On the contrary, the large-scale production of tetrahydrofuran diminishes its cost to 62 \$/kg (99% assay, Chem Impex Ltd., Wood Dale, IL 60191, USA). That is a 52% abatement of its cost. Likewise, dimethylformamide (DMF), a widely utilized industrial solvent that poses moderate acute toxicity and has been detected in the effluents from sewage treatment plants, costs 32 \$/kg for large-scale operation purposes whereas other providers declare values of 1.65–1.8 \$/kg. Hence, a considerable drop of 85% from the lab-scale cost (206.8 \$/kg) is observed.

As shown in Figure 14 the above-mentioned solvents are possible candidates for the industrial implementation of the FA dehydrogenation process owing to their relatively low price, with PC being the most viable choice, due to its eco-friendly characteristics. The cost of dimethyl sulfoxide (DMSO), a non-toxic organic solvent with an adequately high boiling point (189 °C) which presents low acute and chronic toxicity, rises up to 281.7 \$/kg for lab-scale usage (assay $\geq 99.9\%$, ACS reagent) when the corresponding industrial-grade is estimated at around 24 \$/kg.

Studies have demonstrated toxicity issues might rise for these solvents, despite their reasonable pricing. At this point, it should be highlighted that the cost-cutting arising from the large-scale production of DMSO is only 38%, indicating that their insertion into large-scale hydrogen production is not eligible despite its tolerable toxicity. Toluene follows a reverse trend. More precisely, while Thermo Fisher Scientific provides the reagent grade of FA with $\geq 98\%$ assay (Honeywell Fluka™) at the price of 182.4 \$/kg, concurrently, a

supplier from India (Otto Chemie Pvt. Ltd., Mumbai, India) sells the 98–100% assay of FA for industrial use at the price of 21.4 \$/kg. Another provider, Yucheng Jinhe Industrial Co., Ltd., Yucheng town, Shangqiu, Henan, based in China, produces industrial grade of the FA (85% assay) at a much lower price of 0.335 \$/kg.

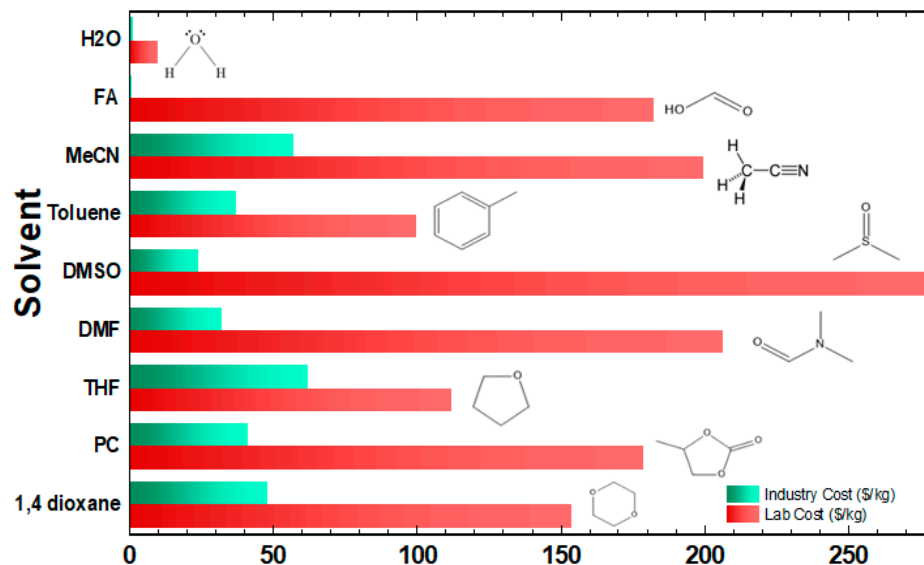


Figure 14. Comparison of the lab-scale and industrial-scale cost of selected solvents for the FA dehydrogenation.

In general, the cost resulting from the FA consumption during the catalytic H₂ production in large-scale implementations is approximately decreased by 88%. Moreover, the high percentages of cost reduction during the transition from the lab scale towards the industrial scale of catalytic FA dehydrogenation procedures highlight the viability of the H₂-based economy.

Next, the cost of the solvent per kg of produced H₂ on different catalytic systems reported in the literature for FA dehydrogenation (Table 4) is discussed. For instance, the catalyst consisting of Ru-PN³ pincer ligand in THF reported by Huang et al. produced 0.02 kg H₂/kg_{solvent} corresponding to TONs of 42,581, as shown in Table 4, Entry #1d. Taking into account that the cost of THF for industrial use is approximately 62\$ per kg, it is estimated that 323\$ for THF is required in order to achieve the production of 1 kg of H₂ by applying this particular catalytic system [101]. In another example, Milstein and co-workers prepared the catalyst Fe-PNP which yielded 19.47 L of H₂ (TONs = 79,632) using 2 mL of THF as the solvent medium. In this case, the expenditure arising from THF is measured as approximately 6.9\$ per 1 kg of produced H₂ [68].

H₂O, being a natural resource, is by definition a free commodity. However, its collection, storage, and distribution have a cost that must be covered in some way. Its price is largely determined by the geographical, geological, and economic factors of the communities where it is produced and where its price is decided. Thus, the price of H₂O can range from a few cents to \$5 per cubic meter, and in exceptional situations much more [136]. For the prevention of catalyst deterioration, high-purity water (deionized or milli-Q) is required, rendering its cost higher. In our calculations, we chose the average price of 11 \$/kg, by Cymitquímica Ltd., Barcelona, Spain, company. A Fe-PNP catalyst has been tested in various solvents, i.e., 1,4 dioxane, THF, PC, and H₂O [68]. Although the price of the H₂O was the lowest, the low activity (0.13 kg H₂/kg solvent) determined the final price as 8.3 \$/kg H₂.

Table 4. Cost analysis based on the solvent.

Entry	Solvent	Conditions	TONs	Cost (\$/kg _{solvent})	kgH ₂ /kg _{solvent}	² \$/kgH ₂ (Solvent)	Ref.
#1	DMSO	1.0 µmol of catalyst FA = 0.3 mL/h, NEt ₃ = 1.50 mL, 0.7 mL DMSO, T = 90 °C	1,100,000	24	0.2	12	[101]
#1a	DMF	1.0 µmol of catalyst FA = 0.3 mL/h, NEt ₃ = 1.50 mL, 10 mL DMSO, T = 90 °C	93,000	32	0.02	161	[101]
#1b	Toluene	1.0 µmol of catalyst FA = 0.3 mL/h, NEt ₃ = 1.50 mL, 10 mL toluene, T = 90 °C	¹ 23,158	37	0.01	343	[101]
#1c	MeCN	1.0 µmol of catalyst FA = 0.3 mL/h, NEt ₃ = 1.50 mL, 5 mL MeCN, T = 90 °C	¹ 55,579	57	0.03	201	[101]
#1d	THF	1.0 µmol of catalyst FA = 0.3 mL/h, NEt ₃ = 1.50 mL, 5 mL THF, T = 90 °C	¹ 42,581	62	0.02	323	[101]
#3	1,4 dioxane	10 µmol catalyst, FA = 3 g, 10.86 mmol NEt ₃ , 2 mL 1,4 dioxane, T = 40 °C	100,000	48	0.97	4.94	[68]
#3b	THF	10 µmol catalyst, FA = 3 g, 10.86 mmol NEt ₃ , 2 mL THF, T = 40 °C	¹ 79,632	62	0.9	6.90	[68]
#3c	PC	10 µmol catalyst, FA = 3 g, 10.86 mmol NEt ₃ , 2 mL PC, T = 40 °C	¹ 47,933	41	0.4	10.3	[68]
#3d	H ₂ O	10 µmol catalyst, FA = 3 g, 10.86 mmol NEt ₃ , 2 mL H ₂ O, T = 40 °C	¹ 12,711	11	0.13	8.3	[68]

¹ the TONs are calculated approximately for continuous operation, using those solvents. ² the cost estimation is compiled by introducing a “scale-factor” that can divide the cost on the order of 10.

3.5. Energy Cost in FA Dehydrogenation

The energy consumption resulting from operating parameters, such as heating and pressurized conditions, is another factor that should be taken into consideration when examining the cost efficiency of the catalytic hydrogen production systems.

Heating of the Catalytic Reactor: The adjustment of the Arrhenius equation to the catalytic systems, $\ln(\text{TOF}) = (-E_{\alpha}/R) \times (1/T) + C$, indicates that the operating temperature determines the H₂ production rate and hence the catalytic performance to a significant extent. Since formic acid dehydrogenation by molecular catalysts is a thermally activated process with high-energy reaction intermediates, an increase in reaction temperature leads to higher hydrogen production rates, i.e., TOFs [98]. As an example, the system [RuCl₂(benzene)]₂/dppe reached TOFs of 92 h⁻¹ at room temperature and achieved a twenty-fold higher TOF number of 1905 h⁻¹ at 40 °C [108]. Considering the abovementioned theoretical and experimental data, applying higher reaction temperatures during FA dehydrogenation would greatly enhance the catalytic performance. However, on the other hand, it would compromise the total cost of the system due to higher energy demands arising from heating. An insightful way to alleviate the heating problem could be the design of low activation energy barrier, E_{α} , systems. The lower the activation energy barrier of the catalytic system, the easier it is to apply lower operating temperatures, along with high performance, less energy consumption, and cost reduction. However, it should be noted that the temperature resulting from fuel cell “waste heat” is usually in the range of 80–90 °C which is desirable and useful for catalytic H₂ production [89].

Pressurized conditions: The evaluation of the viability of the proposed catalytic systems for H₂ production should also include practical parameters, i.e., complexity, safety, and inexpensive storage techniques. The thermodynamic data of the FA dehydrogenation process show that the reaction takes place at ambient temperatures and even at highly

pressurized conditions, due to entropy changes during the process ($\Delta S^\circ = 216 \text{ J/mol}\cdot\text{K}$, $\Delta G^\circ = -32.9 \text{ kJ/mol}$, $\Delta H^\circ = 31.2 \text{ kJ/mol}$) [38,137]. Based on the theoretical calculations and the fact that the FA dehydrogenation reaction is an equilibrium, the maximum pressures of H_2 and CO_2 that can be achieved in neat FA are 225 MPa (2250 bar) [37]. However, the resulting H_2 pressure may have a detrimental effect on the FA conversion under isochoric conditions and the presence of an amine as a consequence of the change in the thermodynamic equilibria [118]. At this point, it should be highlighted that, despite the fact that molecular H_2 has the highest energy content by weight (120 MJ/kg) compared to other fuels, it displays low energy density by volume (0.0108 MJ/L). As a result, the industry has developed conventional methods which allow H_2 storage either as a compressed gas at 100–700 bar or in its liquified form at -253°C [138]. More specifically, the storage of highly pressurized H_2 is achieved by designing mechanical H_2 compressors that increase its volumetric energy density and reduce the tank volume but not its weight. When considering the cost efficiency of the process, the tank volume reduction is a vital factor that contributes to the total cost decrease of the employed catalytic system. In light of the above-mentioned, the same researchers envisioned high-pressure H_2 production for onboard applications and to a greater extent at H_2 gas-filling stations via FA dehydrogenation systems that can operate under high autogenous pressures [37,139,140]. Furthermore, the development of molecular catalysts for the FA dehydrogenation process that exhibit durability at high pressures offers the advantage of separating the generated gas mixture of H_2 and CO_2 . In 2015, Iguchi's group reported a simple phase separation method by decreasing the temperature of the decomposed-FA gas to -51°C . The purified H_2 is then available to feed a fuel cell vehicle without the need for a costly high-pressure pump [58]. Finally, a lot of research has been focused on homogeneous molecular catalysts that are efficient not only for FA dehydrogenation, but also for the reverse reaction of CO_2 hydrogenation, resulting in a "carbon neutral cycle" [55,141]. Owing to the relationship between the water gas shift reaction in the equation $\text{H}_2\text{O} + \text{CO} \leftrightarrow \text{H}_2 + \text{CO}_2 \leftrightarrow \text{HCO}_2\text{H}$, the formation of formic acid is unfavored under ambient conditions. High pressures and the presence of bases are essential during the CO_2 hydrogenation process [141]. Consequently, catalysts that display durability under pressurized conditions or produce autogenous pressures are promising low-priced candidates for both FA dehydrogenation and CO_2 hydrogenation reactions due to their versatile usage [142].

4. Selected Catalytic Systems for Overall-Cost Evaluation

Based on the concept of Section 3, we have made a cost assessment of 10 catalytic systems that could be implemented in the H_2 industry (Table 5). Their selection was based on relatively high TONs, in order for the system to present a reasonable total cost ($\text{\$/kgH}_2$). In spite of the high price of metal precursors ($\text{\$/kg}_{\text{metal precursor}}$), in the majority of the selected systems, the final cost ($\text{\$/kg H}_2$) seems to be influenced by the *ligand* selection. For completeness, we have included the contribution of FA to the total cost. Having selected as the minimum purity the 98% industrial-grade FA with $\sim 600 \text{ \$/ton}$, this has not a very high contribution to the final assessment with a range between 0.0004 and $1.50 \text{ \$/kg H}_2$. In Entry #1, an unsymmetrically protonated PN^3 -pincer complex in conjunction with a Ru metal, NEt_3 additive, and the polar solvent DMSO, was employed for the selective generation of H_2 . The relatively high $\text{\$/kg H}_2$ of (2,6-Bis(di-tert-butylphosphinomethyl)pyridine) ligand, gauges the total cost to $\sim 19 \text{ \$/kg H}_2$. In the same way, the analogous pincer-type catalyst with the cheaper Fe precursor (Entry #3, Table 5) presents a higher total cost of $41.72 \text{ \$/kg H}_2$, as a consequence of the higher price of the Bis(di-tert-butylphosphinomethyl)pyridine ligand ($158,400 \text{ \$/kg}_{\text{ligand}}$). Although both Entry 1# and #3 use the same ligand, the lower performance of #3 ($0.04 \text{ kg H}_2/\text{kg}_{\text{ligand}}$) vs. #1 ($1.50 \text{ kg H}_2/\text{kg}_{\text{ligand}}$) contributes to the higher price.

Table 5. Cost assessment of selected catalytic systems.

Catalytic System	Cost (\$/kgH ₂) Metal	Cost (\$/kgH ₂) Ligand	Cost (\$/kgH ₂) Additive	Cost (\$/kgH ₂) FA	Cost (\$/kgH ₂) Solvent	¹ Total Cost (\$/kgH ₂)	Ref.
#1	0.86	11.9	3.11	0.04	2.85	18.85	[101]
#2	0.55	6.43	0.00	1.61	0.00	8.60	[102]
#3	0.64	31.31	3.46	1.38	4.94	41.72	[68]
#4	0.08	0.81	0.05	0.0004	0.13	1.06	[71]
#5	4.07	1.79	0.00	0.029	0.74	6.82	[44]
#6	1.95	32.98	0.00	1.38	0.32	36.62	[65]
#7	1.94	28.94	0.00	1.21	0.76	32.85	[56]
#8	3.73	3.91	0.45	1.38	0.00	9.46	[119]
#9	1.6	0.33	8.00	1.50	0.00	11.44	[49]
#10	11.28	20.31	3.58	1.38	12.06	48.63	[104]

¹ the cost estimation is compiled by introducing a “scale-factor” that can divide the cost on the order of 10.

Another non-noble-metal catalyst, with the expensive LiBF₄ cocatalyst (3760 \$/kg_{additive}), presents the lowest price, 1.06 \$/kg H₂. To the best of our knowledge, this is the highest performance of a non-noble metal complex, *in tandem* with the low cost. Unfortunately, the highest TONs could be succeeded only with a very low catalyst loading of 0.0001% mol, making it unlikely to be implemented in industry. Higher concentrations contributed to a 30% decrease in the final yield. The most effective Ir N,N-bidentate complexes give outstanding performance, but the relatively high price of [Cp*IrCl₂]₂ metal precursor (245,108 \$/kg_{metal precursor}) leads to higher total cost (\$/kg H₂). Examples include the entries #6 and #7. The Ir complex of 4,7-Dihydroxy-1,10-phenanthroline and 2,3-Piperazinedione dioxime presents the highest stability (TONs > 5,000,000), but higher prices with 33 \$/kg H₂ and 29 \$/kg H₂. Towards this direction, the work of Milstein [102] and Williams [119] using a Ru-9H-acridine pincer complex and an Ir-2-((di-*t*-butylphosphino)methyl)pyridine catalyst is very important. Despite the very high price of 4,5-bis(bromomethyl)acridine ligand (599,900 \$/kg_{ligand}) (Entry #2) and [Ir(1,5-cod)Cl]₂ metal precursor (240,000 \$/kg_{metal precursor}, Entry #8), their excellent TONs afforded a final value of 8.6 \$/kg H₂ and 9.5 \$/kg H₂, respectively. The mixing of commercial [RuCl₂(benzene)]₂ and dppe ligand into a FA/DMOA mixture yielded 467 L H₂ after a lifetime of 1 month. The final cost is 11.44 \$/kg H₂, with the amine, giving an increase of 8 \$. Major drawbacks of additives are the increase of the final cost, in addition to the diminution of volumetric and gravimetric H₂ density. Thus, the designing of additive-free catalytic systems is of great importance. Li and co-workers used an Ir- 2,2'-bi-imidazoline complex, which presents excellent activity and stability (Entry #5) [44] affording a final total cost of 6.82 \$/kg H₂. Other additive-free studies with non-noble metals include the research work of Beller [70] et al. and Tondrau et al. [72]. Their relatively low TONs lead to a high total cost per kg of H₂ produced (209.6 \$/kg H₂ and 12,437 \$/kg H₂, respectively).

In Figure 15, we present an overall-assessment polygon, for the 10 systems described in Table 5. In each of them, the *relative* contribution of each component (metal, ligand, solvent, FA, additive) to the final price (\$/kg H₂) is presented. From this, it becomes evident that: (i) in most cases the ligand cost is the determinant (with an average percentage greater than 60%, Figure 15b); (ii) the cost of additives or solvents may become important at comparative levels; (iii) the metal can be a prominent cost-contributor, although in our case studies only in systems #5 and #9; and (iv) FA, at today's market price, contributes ~20% of the operational cost to the final price (\$/kg H₂) (Figure 15c).

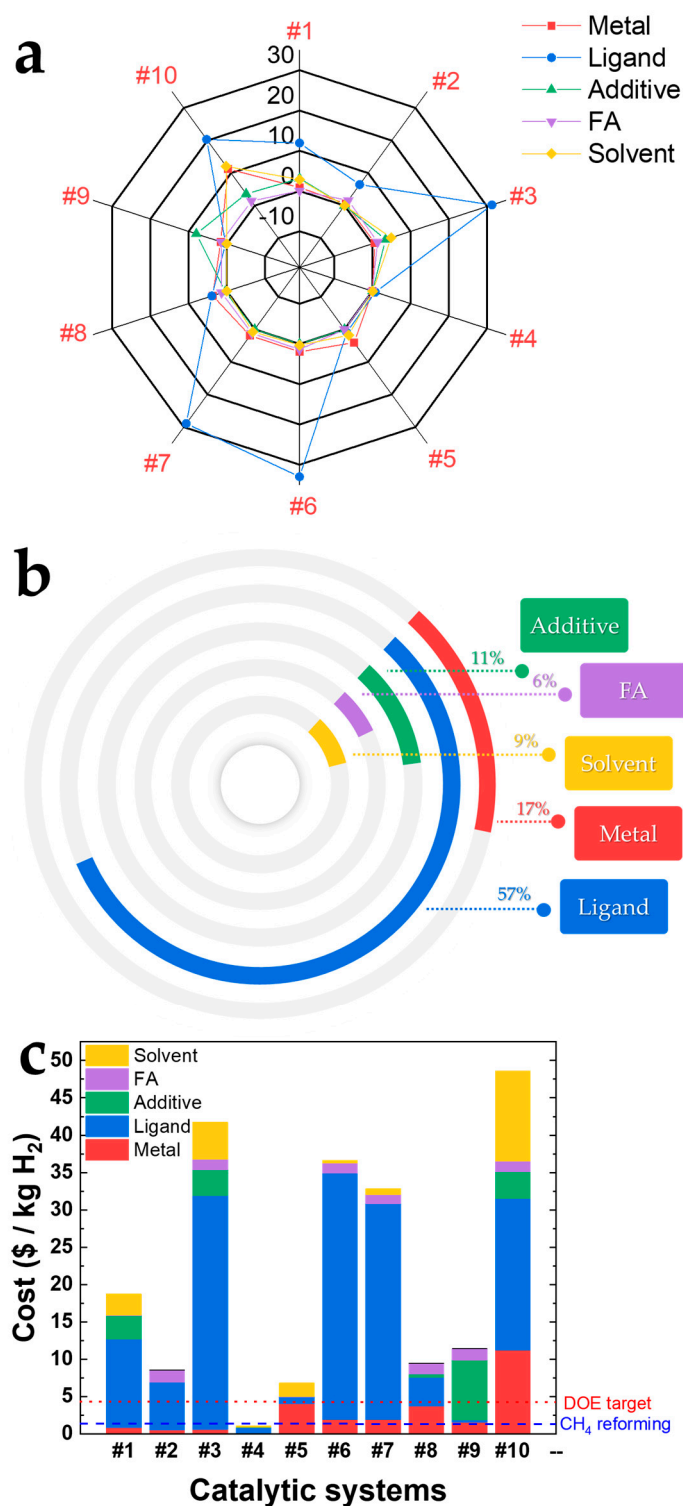


Figure 15. (a) Contribution of several factors (Metal, ligand, additive, FA, solvent) to the final price (\$/kg H₂) of ten selected catalytic systems (b) Average percentage participation of each factor in the total system cost, (c) Bar graphs of ten catalytic systems. Red line: DOE target (4 \$/kg H₂), Blue line: CH₄ reforming price (1.48 \$/kg H₂).

5. Conclusions and Future Perspectives

H₂ as a future energy carrier is a viable option for the replacement of existing fossil fuels. The limitation of low-energy content by volume could be bypassed using LOHCs. Among them, FA is a low-toxic and ecologically benign liquid with a high volumetric

capacity of 53 g H₂/L. The existing gasoline infrastructure can be adapted for FA without incurring additional costs related to handling and distribution. It is true that a lot of integrated FA HFCs devices have been developed. For example, the first functioning indirect formic acid fuel cell that does not need continuous feed gas purification was developed by the group of Czaun [143] using an Ir complex. Laurentzy et al. built a FA PEMFC device, which can produce 7000 kWh/y with electrical efficiency > 45%, with a Ru(H₂O)₆(tos)₂ precursor and TPPTs ligand [41,43]. In another application, DENs startup company [144] together with the Pidko research group [30] implemented a Ru-PNP 25 W catalytic system in a H₂-powered city bus. In their recent review, they conclude that economic viability continues to be a significant barrier to the widespread use of FA-based H₂ storage devices, predicting a \$100,000 total cost, with FC contributing 10% and the catalyst precursor, 1%. Despite the fact that FA-HFCs' penetration is in the future energy market, there are still limitations that should be addressed. Vehicle implementation of a catalytic system requires the following: high selectivity (producing only CO₂ and H₂, with CO in the ppb range), TONs > 1,000,000, TOFs in the order of thousands, and low cost. The cost, as a function of four parameters, including the metal precursor, ligand, additive, and solvent, was analyzed in the present review. Although the less abundant but more efficient noble metals (Ru, Ir, Rh) are costly, the ligand contributes most to the final cost. Concerning the H₂ production cost, according to DOE, the 2023 price is 4\$/kg H₂, while for 2025 and 2030 it is set to be \$2/kg H₂ and \$1/kg H₂, respectively [145]. The economically most favorable ways for H₂ production are steam methane reforming (1.48 \$/kg H₂), coal gasification (1.63 \$/kg H₂), and biomass gasification (1.77 \$/kg H₂) [146]. According to a recent technical report of NREL, a target price for FCEVs is 5 \$/kg H₂ [147], while together with the refueling station utilization, the cost will further increase to 15\$–25 \$/kg H₂ [148]. K.-W. Huang reviews set a threshold price of 16.5 \$/kg H₂ for the calculation of the CON value [23]. Herein, setting a minimum price of 20 \$/kg H₂, economically viable seem to be systems #2, #4, #5, #8, and #9. The cheap non-noble Fe-pincer catalytic system presents the highest efficiency, along with lower price (1.06 \$/kg H₂) [71]. Unfortunately, the highest performance is attained only with a very low concentration of the catalyst (lower than 0.0001% mol), making it very difficult implement in the automobile industry (requires large volume reactors). In some entries, e.g., #9 and #3, the cost of additive could not be negligible and the exploitation of catalysts that could operate without the use of them is quite difficult and acquired only with expensive ligands, e.g., in the case of entry #2. The Ru-acridine additive-free catalyst was very effective but the ligand had the higher contribution to the final cost with 6.43 \$/kg H₂. A solution to a less sophisticated ligand-centered catalyst, where the additive cannot be eliminated, is the replacement of it with solid co-catalysts, e.g., H₂N@SiO₂ particles [53,110]. More desirably, co-catalysts are utilized at lower stoichiometry to the catalyst concentrations, unlike additives that are added in huge amounts, and they can be reused in consecutive catalytic cycles [110]. Another factor that determines the economic viability of a catalytic system is the choice of solvent. In contrast with the, metal precursors and ligands, available only with lab-scale budgets, they could be supplied by several companies at an industrial-scale price. However, as it turned out according to our analysis, in Entries #1, #3, and #10, the solvent price could not be ignored for the final calculation of the \$/kg H₂ cost. The ideal scenario is the catalyst to be dissolved in neat FA, eliminating the use of solvents. However, limitations, such as low solubility, deterioration of the complex because of low pH, and high activation energy, should be addressed. Lastly, a critical point remains the price of FA. Today's industrial-grade FA price ranges between 550\$ and 600 \$/ton [29]. Undoubtedly, there are several examples where high purity FA is required (>98%). The sensitive Fe-PNP catalyst, despite its low non-noble metal catalyst price, could be deactivated in industrial-grade FA, increasing the overall cost (Entry #6). In addition, continuous operation requires high volumes where the low-purity FA can accumulate H₂O, something that is detrimental for some catalysts, even if at low concentrations [149]. In order for the cost of pure FA to be economically viable according to DOE standards, the price needs to drop to approximately 200\$/ton [23]. This price could be

achievable through future CCS and CCU technology [150]. To evaluate the possibilities and limitations of future developments, engineering infrastructure must be taken into account. The FA dehydrogenation scenario might potentially contribute to the future of H₂ energy, and the adventure has just begun. It is time to convert hurdles into aspirations.

Author Contributions: Writing—original draft preparation, Data curation, M.S.; writing—original draft preparation, figure illustration, A.G.; writing—original draft preparation, G.K.; writing—original draft preparation, M.T.; conceptualization, writing—review and editing, Y.D.; conceptualization, writing—review and editing, supervision, funding acquisition, M.L. All authors have read and agreed to the published version of the manuscript.

Funding: The research project was supported by the Hellenic Foundation for Research and Innovation (H.F.R.I.) under the “2nd Call for H.F.R.I. Research Projects to support Faculty Members & Researchers” (Project Number: 3832).

Conflicts of Interest: The authors declare no conflict of interest.

References

- World Energy Balances. Available online: <https://www.iea.org/data-and-statistics/data-product/world-energy-balances> (accessed on 1 January 2023).
- The Evidence Is Clear: The Time for Action Is Now. We Can Halve Emissions by 2030. Available online: <https://www.ipcc.ch/2022/04/04/ipcc-ar6-wgiii-pressrelease/> (accessed on 30 December 2022).
- Quarton, C.J.; Tlili, O.; Welder, L.; Mansilla, C.; Blanco, H.; Heinrichs, H.; Leaver, J.; Samsatli, N.J.; Lucchese, P.; Robinius, M.; et al. The curious case of the conflicting roles of hydrogen in global energy scenarios. *Sustain. Energy Fuels* **2020**, *4*, 80–95. [\[CrossRef\]](#)
- Pivovar, B.; Rustagi, N.; Satyapal, S. Hydrogen at Scale (H₂ @Scale): Key to a Clean, Economic, and Sustainable Energy System. *Electrochem. Soc. Interface* **2018**, *27*, 47–52. [\[CrossRef\]](#)
- Hanley, E.S.; Deane, J.P.; Gallachóir, B.P.Ó. The role of hydrogen in low carbon energy futures—A review of existing perspectives. *Renew. Sustain. Energy Rev.* **2018**, *82*, 3027–3045. [\[CrossRef\]](#)
- Yue, M.; Lambert, H.; Pahon, E.; Roche, R.; Jemei, S.; Hissel, D. Hydrogen energy systems: A critical review of technologies, applications, trends and challenges. *Renew. Sustain. Energy Rev.* **2021**, *146*, 111180. [\[CrossRef\]](#)
- Abe, J.O.; Popoola, A.P.I.; Ajenifuja, E.; Popoola, O.M. Hydrogen energy, economy and storage: Review and recommendation. *Int. J. Hydrogen Energy* **2019**, *44*, 15072–15086. [\[CrossRef\]](#)
- Anandarajah, G.; McDowall, W.; Ekins, P. Decarbonising road transport with hydrogen and electricity: Long term global technology learning scenarios. *Int. J. Hydrogen Energy* **2013**, *38*, 3419–3432. [\[CrossRef\]](#)
- Ruffini, E.; Wei, M. Future costs of fuel cell electric vehicles in California using a learning rate approach. *Energy* **2018**, *150*, 329–341. [\[CrossRef\]](#)
- Hydrogen Refuelling Stations Worldwide. Available online: <https://www.h2stations.org/> (accessed on 21 December 2022).
- Hua, T.; Ahluwalia, R.; Eudy, L.; Singer, G.; Jermer, B.; Asselin-Miller, N.; Wessel, S.; Patterson, T.; Marcinkoski, J. Status of hydrogen fuel cell electric buses worldwide. *J. Power Source* **2014**, *269*, 975–993. [\[CrossRef\]](#)
- Alstom Coradia iLint Distance Run. Available online: <https://www.alstom.com/alstom-coradia-ilint-distance-run> (accessed on 15 November 2022).
- Zhang, F.; Zhao, P.; Niu, M.; Maddy, J. The survey of key technologies in hydrogen energy storage. *Int. J. Hydrogen Energy* **2016**, *41*, 14535–14552. [\[CrossRef\]](#)
- Schmidt, O.; Gambhir, A.; Staffell, I.; Hawkes, A.; Nelson, J.; Few, S. Future cost and performance of water electrolysis: An expert elicitation study. *Int. J. Hydrogen Energy* **2017**, *42*, 30470–30492. [\[CrossRef\]](#)
- Quarton, C.J.; Samsatli, S. The value of hydrogen and carbon capture, storage and utilisation in decarbonising energy: Insights from integrated value chain optimisation. *Appl. Energy* **2020**, *257*, 113936. [\[CrossRef\]](#)
- Lang, C.; Jia, Y.; Yao, X. Recent advances in liquid-phase chemical hydrogen storage. *Energy Storage Mater.* **2020**, *26*, 290–312. [\[CrossRef\]](#)
- Hwang, H.T.; Varma, A. Hydrogen storage for fuel cell vehicles. *Curr. Opin. Chem. Eng.* **2014**, *5*, 42–48. [\[CrossRef\]](#)
- Alazemi, J.; Andrews, J. Automotive hydrogen fuelling stations: An international review. *Renew. Sustain. Energy Rev.* **2015**, *48*, 483–499. [\[CrossRef\]](#)
- Suh, M.P.; Park, H.J.; Prasad, T.K.; Lim, D.-W. Hydrogen Storage in Metal–Organic Frameworks. *Chem. Rev.* **2012**, *112*, 782–835. [\[CrossRef\]](#)
- Sordakis, K.; Tang, C.; Vogt, L.K.; Junge, H.; Dyson, P.J.; Beller, M.; Laurenczy, G. Homogeneous Catalysis for Sustainable Hydrogen Storage in Formic Acid and Alcohols. *Chem. Rev.* **2018**, *118*, 372–433. [\[CrossRef\]](#)
- Viswanathan, B. Hydrogen Storage. In *Energy Sources*; Elsevier: Amsterdam, The Netherlands, 2017; pp. 185–212. [\[CrossRef\]](#)
- Xu, R.; Lu, W.; Toan, S.; Zhou, Z.; Russell, C.K.; Sun, Z.; Sun, Z. Thermocatalytic formic acid dehydrogenation: Recent advances and emerging trends. *J. Mater. Chem. A* **2021**, *9*, 24241–24260. [\[CrossRef\]](#)

23. Dutta, I.; Chatterjee, S.; Cheng, H.; Parsapur, R.K.; Liu, Z.; Li, Z.; Ye, E.; Kawanami, H.; Low, J.S.C.; Lai, Z.; et al. Formic Acid to Power towards Low-Carbon Economy. *Adv. Energy Mater.* **2022**, *12*, 2103799. [CrossRef]
24. Hydrogen and Fuel Cell Technologies Office DOE Technical Targets for Onboard Hydrogen Storage for Light-Duty Vehicles. Available online: <https://www.energy.gov/eere/fuelcells/doe-technical-targets-onboard-hydrogen-storage-light-duty-vehicles> (accessed on 25 November 2022).
25. Álvarez, A.; Bansode, A.; Urakawa, A.; Bavykina, A.V.; Wezendonk, T.A.; Makkee, M.; Gascon, J.; Kapteijn, F. Challenges in the Greener Production of Formates/Formic Acid, Methanol, and DME by Heterogeneously Catalyzed CO₂ Hydrogenation Processes. *Chem. Rev.* **2017**, *117*, 9804–9838. [CrossRef]
26. Staffell, I.; Scamman, D.; Velazquez Abad, A.; Balcombe, P.; Dodds, P.E.; Ekins, P.; Shah, N.; Ward, K.R. The role of hydrogen and fuel cells in the global energy system. *Energy Environ. Sci.* **2019**, *12*, 463–491. [CrossRef]
27. Toyota MIRAI, MIRAI Means ‘The Future’. Available online: <https://h2.live/en/fuelcell-cars/toyota-mirai/> (accessed on 23 October 2022).
28. Formic Acid Market—Growth, Trends, COVID-19 Impact, and Forecasts (2023–2028). Available online: <https://www.mordorintelligence.com/industry-reports/formic-acid-market> (accessed on 28 November 2022).
29. Formic Acid Market by Product Types (Grades of 85%, 94%, 99%, and Others), Applications (Agriculture, Leather & Textile, Rubber, Chemical & Pharmaceuticals, and Others), and Regions (Asia Pacific, North America, Latin America, Europe, and Middle East & Africa)—Global Industry Analysis, Growth, Share, Size, Trends, and Forecast, 2021–2028. Available online: <https://dataintelo.com/report/formic-acid-market/> (accessed on 29 November 2022).
30. van Putten, R.; Wissink, T.; Swinkels, T.; Pidko, E.A. Fuelling the hydrogen economy: Scale-up of an integrated formic acid-to-power system. *Int. J. Hydrogen Energy* **2019**, *44*, 28533–28541. [CrossRef]
31. Singh, A.K.; Singh, S.; Kumar, A. Hydrogen energy future with formic acid: A renewable chemical hydrogen storage system. *Catal. Sci. Technol.* **2016**, *6*, 12–40. [CrossRef]
32. Czaun, M.; Goeppert, A.; Kothandaraman, J.; May, R.B.; Haiges, R.; Prakash, G.K.S.; Olah, G.A. Formic Acid as a Hydrogen Storage Medium: Ruthenium-Catalyzed Generation of Hydrogen from Formic Acid in Emulsions. *ACS Catal.* **2013**, *4*, 311–320. [CrossRef]
33. Yu, X.; Pickup, P.G. Recent advances in direct formic acid fuel cells (DFAFC). *J. Power Source* **2008**, *182*, 124–132. [CrossRef]
34. Rejal, S.Z.; Masdar, M.S.; Kamarudin, S.K. A parametric study of the direct formic acid fuel cell (DFAFC) performance and fuel crossover. *Int. J. Hydrogen Energy* **2014**, *39*, 10267–10274. [CrossRef]
35. Han, D.; Tsipoaka, M.; Shanmugam, S. A modified cathode catalyst layer with optimum electrode exposure for high current density and durable proton exchange membrane fuel cell operation. *J. Power Sources* **2021**, *496*, 229816. [CrossRef]
36. Chang, J.; Feng, L.; Liu, C.; Xing, W.; Hu, X. An Effective Pd-Ni₂P/C Anode Catalyst for Direct Formic Acid Fuel Cells. *Angew. Chem. Int. Ed.* **2014**, *53*, 122–126. [CrossRef]
37. Eppinger, J.; Huang, K.-W. Formic Acid as a Hydrogen Energy Carrier. *ACS Energy Lett.* **2017**, *2*, 188–195. [CrossRef]
38. Guan, C.; Pan, Y.; Zhang, T.; Ajitha, M.J.; Huang, K.-W. An Update on Formic Acid Dehydrogenation by Homogeneous Catalysis. *Chem. Asian J.* **2020**, *15*, 937–946. [CrossRef]
39. U.S. Department of Energy. Technology Readiness Assessment Guide. Available online: <https://www.directives.doe.gov/directives-documents/400-series/0413.3-EGuide-04/@images/file> (accessed on 21 October 2022).
40. What Are Technology Readiness Levels (TRL)? Available online: <https://www.twi-global.com/technical-knowledge/faqs/technology-readiness-levels> (accessed on 29 December 2022).
41. Gabor, L.; Céline, F.; Paul, D. Hydrogen Production from Formic Acid. EP 1 918 247 A1. 7 May 2008. Available online: <https://patentimages.storage.googleapis.com/02/4b/0e/db9b2f842c2658/EP1918247A1.pdf> (accessed on 20 October 2022).
42. Huang, K.-W.; Zheng, J. Electricity Generation Devices Using Formic Acid. WO 2017/103820 A1. 22 June 2017. Available online: <https://repository.kaust.edu.sa/bitstream/handle/10754/625325/WO2017103820A1.pdf?sequence=1&isAllowed=y> (accessed on 20 October 2022).
43. The world’s First Formic Acid-Based Fuel Cell. Available online: <https://actu.epfl.ch/news/the-world-s-first-formic-acid-based-fuel-cell/> (accessed on 12 November 2022).
44. Wang, Z.; Lu, S.-M.; Li, J.; Wang, J.; Li, C. Unprecedentedly High Formic Acid Dehydrogenation Activity on an Iridium Complex with an N,N′-Diimine Ligand in Water. *Chem. Eur. J.* **2015**, *21*, 12592–12595. [CrossRef]
45. Belkova, N.V.; Filippov, O.A.; Osipova, E.S.; Safronov, S.V.; Epstein, L.M.; Shubina, E.S. Influence of phosphine (pincer) ligands on the transition metal hydrides reactivity. *Coord. Chem. Rev.* **2021**, *438*, 213799. [CrossRef]
46. Iglesias, M.; Oro, L.A. Mechanistic Considerations on Homogeneously Catalyzed Formic Acid Dehydrogenation. *Eur. J. Inorg. Chem.* **2018**, *2018*, 2125–2138. [CrossRef]
47. Mellmann, D.; Sponholz, P.; Junge, H.; Beller, M. Formic acid as a hydrogen storage material—Development of homogeneous catalysts for selective hydrogen release. *Chem. Soc. Rev.* **2016**, *45*, 3954–3988. [CrossRef]
48. Gao, Y.; Kuncheria, J.; Puddephatt, R.J.; Yap, G.P.A. An efficient binuclear catalyst for decomposition of formic acid. *Chem. Commun.* **1998**, 2365–2366. [CrossRef]
49. Sponholz, P.; Mellmann, D.; Junge, H.; Beller, M. Towards a Practical Setup for Hydrogen Production from Formic Acid. *ChemSuschem* **2013**, *6*, 1172–1176. [CrossRef]

50. Fellay, C.; Yan, N.; Dyson, P.J.; Laurenczy, G. Selective Formic Acid Decomposition for High-Pressure Hydrogen Generation: A Mechanistic Study. *Chem. Eur. J.* **2009**, *15*, 3752–3760. [\[CrossRef\]](#)
51. Filonenko, G.; van Putten, R.; Schulpen, E.N.; Hensen, E.J.M.; Pidko, E. Highly Efficient Reversible Hydrogenation of Carbon Dioxide to Formates Using a Ruthenium PNP-Pincer Catalyst. *Chemcatchem* **2014**, *6*, 1526–1530. [\[CrossRef\]](#)
52. Prichatz, C.; Trincado, M.; Tan, L.; Casas, F.; Kammer, A.; Junge, H.; Beller, M.; Grützmacher, H. Highly Efficient Base-Free Dehydrogenation of Formic Acid at Low Temperature. *ChemSuschem* **2018**, *11*, 3092–3095. [\[CrossRef\]](#)
53. Solakidou, M.; Theodorakopoulos, M.; Deligiannakis, Y.; Louludi, M. Double-ligand Fe, Ru catalysts: A novel route for enhanced H₂ production from Formic Acid. *Int. J. Hydrogen Energy* **2020**, *45*, 17367–17377. [\[CrossRef\]](#)
54. Theodorakopoulos, M.; Solakidou, M.; Deligiannakis, Y.; Louludi, M. A Use-Store-Reuse (USR) Concept in Catalytic HCOOH Dehydrogenation: Case-Study of a Ru-Based Catalytic System for Long-Term USR under Ambient O₂. *Energies* **2021**, *14*, 481. [\[CrossRef\]](#)
55. Himeda, Y. Highly efficient hydrogen evolution by decomposition of formic acid using an iridium catalyst with 4,4'-dihydroxy-2,2'-bipyridine. *Green Chem.* **2009**, *11*, 2018–2022. [\[CrossRef\]](#)
56. Lu, S.-M.; Wang, Z.; Wang, J.; Li, J.; Li, C. Hydrogen generation from formic acid decomposition on a highly efficient iridium catalyst bearing a diaminoglyoxime ligand. *Green Chem.* **2018**, *20*, 1835–1840. [\[CrossRef\]](#)
57. Wang, W.-H.; Ertem, M.Z.; Xu, S.; Onishi, N.; Manaka, Y.; Suna, Y.; Kambayashi, H.; Muckerman, J.T.; Fujita, E.; Himeda, Y. Highly Robust Hydrogen Generation by Bioinspired Ir Complexes for Dehydrogenation of Formic Acid in Water: Experimental and Theoretical Mechanistic Investigations at Different pH. *ACS Catal.* **2015**, *5*, 5496–5504. [\[CrossRef\]](#)
58. Iguchi, M.; Himeda, Y.; Manaka, Y.; Matsuoka, K.; Kawanami, H. Simple Continuous High-Pressure Hydrogen Production and Separation System from Formic Acid under Mild Temperatures. *Chemcatchem* **2016**, *8*, 886–890. [\[CrossRef\]](#)
59. Wang, S.; Huang, H.; Roisnel, T.; Bruneau, C.; Fischmeister, C. Base-Free Dehydrogenation of Aqueous and Neat Formic Acid with Iridium(III) Cp*(dipyridylamine) Catalysts. *ChemSuschem* **2019**, *12*, 179–184. [\[CrossRef\]](#)
60. Mo, X.-F.; Liu, C.; Chen, Z.-W.; Ma, F.; He, P.; Yi, X.-Y. Metal–Ligand Cooperation in Cp*Ir-Pyridylpyrrole Complexes: Rational Design and Catalytic Activity in Formic Acid Dehydrogenation and CO₂ Hydrogenation under Ambient Conditions. *Inorg. Chem.* **2021**, *60*, 16584–16592. [\[CrossRef\]](#)
61. Cheng, S.; Lang, Z.; Du, J.; Du, Z.; Li, Y.; Tan, H.; Li, Y. Engineering of iridium complexes for the efficient hydrogen evolution of formic acid without additives. *J. Catal.* **2022**, *413*, 119–126. [\[CrossRef\]](#)
62. Jongbloed, L.S.; de Bruin, B.; Reek, J.N.H.; Lutz, M.; van der Vlugt, J.I. Reversible cyclometalation at RhI as a motif for metal–ligand bifunctional bond activation and base-free formic acid dehydrogenation. *Catal. Sci. Technol.* **2016**, *6*, 1320–1327. [\[CrossRef\]](#)
63. Fink, C.; Laurenczy, G. A Precious Catalyst: Rhodium-Catalyzed Formic Acid Dehydrogenation in Water. *Eur. J. Inorg. Chem.* **2019**, *2019*, 2381–2387. [\[CrossRef\]](#)
64. Hermosilla, P.; Urriolabeitia, A.; Iglesias, M.; Polo, V.; Casado, M. Efficient solventless dehydrogenation of formic acid by a CNC-based rhodium catalyst. *Inorg. Chem. Front.* **2022**, *9*, 4538–4547. [\[CrossRef\]](#)
65. Iguchi, M.; Himeda, Y.; Manaka, Y.; Kawanami, H. Development of an Iridium-Based Catalyst for High-Pressure Evolution of Hydrogen from Formic Acid. *ChemSuschem* **2016**, *9*, 2749–2753. [\[CrossRef\]](#)
66. Zweig, J.E.; Kim, D.E.; Newhouse, T.R. Methods Utilizing First-Row Transition Metals in Natural Product Total Synthesis. *Chem. Rev.* **2017**, *117*, 11680–11752. [\[CrossRef\]](#)
67. Tamang, S.R.; Findlater, M. Emergence and Applications of Base Metals (Fe, Co, and Ni) in Hydroboration and Hydrosilylation. *Molecules* **2019**, *24*, 3194. [\[CrossRef\]](#)
68. Zell, T.; Butschke, B.; Ben-David, Y.; Milstein, D. Efficient Hydrogen Liberation from Formic Acid Catalyzed by a Well-Defined Iron Pincer Complex under Mild Conditions. *Chem. Eur. J.* **2013**, *19*, 8068–8072. [\[CrossRef\]](#)
69. Boddien, A.; Loges, B.; Gärtner, F.; Torborg, C.; Fumino, K.; Junge, H.; Ludwig, R.; Beller, M. Iron-Catalyzed Hydrogen Production from Formic Acid. *J. Am. Chem. Soc.* **2010**, *132*, 8924–8934. [\[CrossRef\]](#)
70. Boddien, A.; Mellmann, D.; Gärtner, F.; Jackstell, R.; Junge, H.; Dyson, P.J.; Laurenczy, G.; Ludwig, R.; Beller, M. Efficient Dehydrogenation of Formic Acid Using an Iron Catalyst. *Science* **2011**, *333*, 1733–1736. [\[CrossRef\]](#)
71. Bielinski, E.A.; Lagaditis, P.O.; Zhang, Y.; Mercado, B.Q.; Würtele, C.; Bernskoetter, W.H.; Hazari, N.; Schneider, S. Lewis Acid-Assisted Formic Acid Dehydrogenation Using a Pincer-Supported Iron Catalyst. *J. Am. Chem. Soc.* **2014**, *136*, 10234–10237. [\[CrossRef\]](#)
72. Tondreau, A.M.; Boncella, J.M. 1,2-Addition of Formic or Oxalic Acid to [−]N{CH₂CH₂(PiPr₂)₂}-Supported Mn(I) Dicarbonyl Complexes and the Manganese-Mediated Decomposition of Formic Acid. *Organometallics* **2016**, *35*, 2049–2052. [\[CrossRef\]](#)
73. Léval, A.; Agapova, A.; Steinlechner, C.; Alberico, E.; Junge, H.; Beller, M. Hydrogen production from formic acid catalyzed by a phosphine free manganese complex: Investigation and mechanistic insights. *Green Chem.* **2020**, *22*, 913–920. [\[CrossRef\]](#)
74. Enthaler, S.; Brück, A.; Kammer, A.; Junge, H.; Irran, E.; Güllak, S. Exploring the Reactivity of Nickel Pincer Complexes in the Decomposition of Formic Acid to CO₂/H₂ and the Hydrogenation of NaHCO₃ to HCOONa. *Chemcatchem* **2015**, *7*, 65–69. [\[CrossRef\]](#)
75. Neary, M.C.; Parkin, G. Nickel-catalyzed release of H₂ from formic acid and a new method for the synthesis of zerovalent Ni(PMe₃)₄. *Dalton Trans.* **2016**, *45*, 14645–14650. [\[CrossRef\]](#) [\[PubMed\]](#)
76. Zhou, W.; Wei, Z.; Spannenberg, A.; Jiao, H.; Junge, K.; Junge, H.; Beller, M. Cobalt-Catalyzed Aqueous Dehydrogenation of Formic Acid. *Chem. Eur. J.* **2019**, *25*, 8459–8464. [\[CrossRef\]](#) [\[PubMed\]](#)

77. Loges, B.; Boddien, A.; Junge, H.; Beller, M. Controlled Generation of Hydrogen from Formic Acid Amine Adducts at Room Temperature and Application in H₂/O₂ Fuel Cells. *Angew. Chem. Int. Ed.* **2008**, *47*, 3962–3965. [\[CrossRef\]](#) [\[PubMed\]](#)
78. Tanaka, R.; Yamashita, M.; Chung, L.W.; Morokuma, K.; Nozaki, K. Mechanistic Studies on the Reversible Hydrogenation of Carbon Dioxide Catalyzed by an Ir-PNP Complex. *Organometallics* **2011**, *30*, 6742–6750. [\[CrossRef\]](#)
79. Coffey, R.S. The decomposition of formic acid catalysed by soluble metal complexes. *Chem. Commun.* **1967**, 923b–924. [\[CrossRef\]](#)
80. Nakazawa, H. Chapter 7. Catalysis by Organometallic Complexes. In *Coordination Chemistry Fundamentals*; Nakazawa, H., Koe, J., Eds.; Royal Society of Chemistry: Cambridge, UK, 2021; pp. 85–96. [\[CrossRef\]](#)
81. Miranda, P.E. (Ed.) Hydrogen Storage and Transport by Organic Hydrides and Application of Ammonia. In *Science and Engineering of Hydrogen-Based Energy Technologies*; Elsevier: Amsterdam, The Netherlands, 2019; pp. 229–236. [\[CrossRef\]](#)
82. Wang, W.-H.; Himeda, Y.; Muckerman, J.T.; Manbeck, G.F.; Fujita, E. CO₂ Hydrogenation to Formate and Methanol as an Alternative to Photo- and Electrochemical CO₂ Reduction. *Chem. Rev.* **2015**, *115*, 12936–12973. [\[CrossRef\]](#)
83. Piccirilli, L.; Pinheiro, D.L.J.; Nielsen, M. Recent Progress with Pincer Transition Metal Catalysts for Sustainability. *Catalysts* **2020**, *10*, 773. [\[CrossRef\]](#)
84. Boddien, A.; Loges, B.; Junge, H.; Beller, M. Hydrogen Generation at Ambient Conditions: Application in Fuel Cells. *ChemSuschem* **2008**, *1*, 751–758. [\[CrossRef\]](#)
85. Gan, W.; Snelders, D.J.M.; Dyson, P.J.; Laurenczy, G. Ruthenium(II)-Catalyzed Hydrogen Generation from Formic Acid using Cationic, Ammoniomethyl-Substituted Triarylphosphine Ligands. *Chemcatchem* **2013**, *5*, 1126–1132. [\[CrossRef\]](#)
86. Fellay, C.; Dyson, P.; Laurenczy, G. A Viable Hydrogen-Storage System Based On Selective Formic Acid Decomposition with a Ruthenium Catalyst. *Angew. Chem. Int. Ed.* **2008**, *47*, 3966–3968. [\[CrossRef\]](#)
87. Guerriero, A.; Bricout, H.; Sordakis, K.; Peruzzini, M.; Monflier, E.; Hapiot, F.; Laurenczy, G.; Gonsalvi, L. Hydrogen Production by Selective Dehydrogenation of HCOOH Catalyzed by Ru-Biaryl Sulfonated Phosphines in Aqueous Solution. *ACS Catal.* **2014**, *4*, 3002–3012. [\[CrossRef\]](#)
88. Fukuzumi, S.; Kobayashi, T.; Suenobu, T. Efficient Catalytic Decomposition of Formic Acid for the Selective Generation of H₂ and H/D Exchange with a Water-Soluble Rhodium Complex in Aqueous Solution. *ChemSuschem* **2008**, *1*, 827–834. [\[CrossRef\]](#)
89. Guo, J.; Yin, C.K.; Zhong, D.L.; Wang, Y.L.; Qi, T.; Liu, G.H.; Shen, L.T.; Zhou, Q.S.; Peng, Z.H.; Yao, H.; et al. Formic Acid as a Potential On-Board Hydrogen Storage Method: Development of Homogeneous Noble Metal Catalysts for Dehydrogenation Reactions. *ChemSuschem* **2021**, *14*, 2655–2681. [\[CrossRef\]](#)
90. Morales-Morales, D. (Ed.) *Pincer Compounds: Chemistry and Applications*; Elsevier: Amsterdam, The Netherlands, 2018.
91. Liu, C.-C.; Liu, Q.-L.; Wu, Z.-Y.; Chen, Y.-C.; Xie, H.-J.; Lei, Q.-F.; Fang, W.-J. Mechanistic insights into small molecule activation induced by ligand cooperativity in PCcarbeneP nickel pincer complexes: A quantum chemistry study. *J. Mol. Model.* **2015**, *21*, 242. [\[CrossRef\]](#)
92. Adams, G.M.; Weller, A.S. POP-type ligands: Variable coordination and hemilabile behaviour. *Coord. Chem. Rev.* **2018**, *355*, 150–172. [\[CrossRef\]](#)
93. Gradiski, M.V.; Tsui, B.T.H.; Lough, A.J.; Morris, R.H. PNN' & P₂NN' ligands *via* reductive amination with phosphine aldehydes: Synthesis and base-metal coordination chemistry. *Dalton Trans.* **2019**, *48*, 2150–2159. [\[CrossRef\]](#)
94. Li, H.; Zheng, B.; Huang, K.-W. A new class of PN₃-pincer ligands for metal–ligand cooperative catalysis. *Coord. Chem. Rev.* **2015**, *293–294*, 116–138. [\[CrossRef\]](#)
95. Mellone, I.; Gorgas, N.; Bertini, F.; Peruzzini, M.; Kirchner, K.; Gonsalvi, L. Selective Formic Acid Dehydrogenation Catalyzed by Fe-PNP Pincer Complexes Based on the 2,6-Diaminopyridine Scaffold. *Organometallics* **2016**, *35*, 3344–3349. [\[CrossRef\]](#)
96. Hsu, M.S.S.-F.; Rommel, D.-C.S.; Eversfield, M.S.P.; Muller, K.; Klemm, E.; Thiel, W.R.; Plietker, B. A Rechargeable Hydrogen Battery Based on Ru Catalysis. *Angew. Chem. Int. Ed.* **2014**, *53*, 7074–7078. [\[CrossRef\]](#)
97. Anderson, N.H.; Boncella, J.; Tondreau, A.M. Manganese-Mediated Formic Acid Dehydrogenation. *Chem. Eur. J.* **2019**, *25*, 10557–10560. [\[CrossRef\]](#)
98. Stathi, P.; Solakidou, M.; Louloudi, M.; Deligiannakis, Y. From Homogeneous to Heterogenized Molecular Catalysts for H₂ Production by Formic Acid Dehydrogenation: Mechanistic Aspects, Role of Additives, and Co-Catalysts. *Energies* **2020**, *13*, 733. [\[CrossRef\]](#)
99. Mellone, I.; Bertini, F.; Peruzzini, M.; Gonsalvi, L. An active, stable and recyclable Ru(II) tetraphosphine-based catalytic system for hydrogen production by selective formic acid dehydrogenation. *Catal. Sci. Technol.* **2016**, *6*, 6504–6512. [\[CrossRef\]](#)
100. Bertini, F.; Mellone, I.; Ienco, A.; Peruzzini, M.; Gonsalvi, L. Iron(II) Complexes of the Linear *rac*-Tetraphos-1 Ligand as Efficient Homogeneous Catalysts for Sodium Bicarbonate Hydrogenation and Formic Acid Dehydrogenation. *ACS Catal.* **2015**, *5*, 1254–1265. [\[CrossRef\]](#)
101. Pan, Y.; Pan, C.-L.; Zhang, Y.; Li, H.; Min, S.; Guo, X.; Zheng, B.; Chen, H.; Anders, A.; Lai, Z.; et al. Selective Hydrogen Generation from Formic Acid with Well-Defined Complexes of Ruthenium and Phosphorus–Nitrogen PN₃-Pincer Ligand. *Chem. Asian J.* **2016**, *11*, 1357–1360. [\[CrossRef\]](#) [\[PubMed\]](#)
102. Kar, S.; Rauch, M.; Leitus, G.; Ben-David, Y.; Milstein, D. Highly efficient additive-free dehydrogenation of neat formic acid. *Nat. Catal.* **2021**, *4*, 193–201. [\[CrossRef\]](#)
103. Mellone, I.; Peruzzini, M.; Rosi, L.; Mellmann, D.; Junge, H.; Beller, M.; Gonsalvi, L. Formic acid dehydrogenation catalysed by ruthenium complexes bearing the tripodal ligands triphos and NP₃. *Dalton Trans.* **2013**, *42*, 2495–2501. [\[CrossRef\]](#) [\[PubMed\]](#)

104. Papp, G.; Ölveti, G.; Horváth, H.; Kathó, Á.; Joó, F. Highly efficient dehydrogenation of formic acid in aqueous solution catalysed by an easily available water-soluble iridium(III) dihydride. *Dalton Trans.* **2016**, *45*, 14516–14519. [\[CrossRef\]](#)
105. DuBois, M.R.; DuBois, D.L. The role of pendant bases in molecular catalysts for H₂ oxidation and production. *Comptes Rendus Chim.* **2008**, *11*, 805–817. [\[CrossRef\]](#)
106. Li, X.; Ma, X.; Shi, F.; Deng, Y. Hydrogen Generation from Formic Acid Decomposition with a Ruthenium Catalyst Promoted by Functionalized Ionic Liquids. *Chemsuschem* **2010**, *3*, 71–74. [\[CrossRef\]](#)
107. Kothandaraman, J.; Czaun, M.; Goeppert, A.; Haiges, R.; Jones, J.-P.; May, R.B.; Prakash, G.K.S.; Olah, G.A. Amine-Free Reversible Hydrogen Storage in Formate Salts Catalyzed by Ruthenium Pincer Complex without pH Control or Solvent Change. *Chemsuschem* **2015**, *8*, 1442–1451. [\[CrossRef\]](#)
108. Boddien, A.; Loges, B.; Junge, H.; Gärtner, F.; Noyes, J.R.; Beller, M. Continuous Hydrogen Generation from Formic Acid: Highly Active and Stable Ruthenium Catalysts. *Adv. Synth. Catal.* **2009**, *351*, 2517–2520. [\[CrossRef\]](#)
109. Majewski, A.; Morris, D.J.; Kendall, K.; Wills, M. A Continuous-Flow Method for the Generation of Hydrogen from Formic Acid. *Chemsuschem* **2010**, *3*, 431–434. [\[CrossRef\]](#)
110. Solakidou, M.; Deligiannakis, Y.; Louludi, M. Heterogeneous amino-functionalized particles boost hydrogen production from Formic Acid by a ruthenium complex. *Int. J. Hydrogen Energy* **2018**, *43*, 21386–21397. [\[CrossRef\]](#)
111. Fukuzumi, S.; Kobayashi, T.; Suenobu, T. Unusually Large Tunneling Effect on Highly Efficient Generation of Hydrogen and Hydrogen Isotopes in pH-Selective Decomposition of Formic Acid Catalyzed by a Heterodinuclear Iridium–Ruthenium Complex in Water. *J. Am. Chem. Soc.* **2010**, *132*, 1496–1497. [\[CrossRef\]](#)
112. Grubel, K.; Jeong, H.; Yoon, C.W.; Autrey, T. Challenges and opportunities for using formate to store, transport, and use hydrogen. *J. Energy Chem.* **2020**, *41*, 216–224. [\[CrossRef\]](#)
113. Su, J.; Yang, L.; Lu, M.; Lin, H. Highly Efficient Hydrogen Storage System Based on Ammonium Bicarbonate/Formate Redox Equilibrium over Palladium Nanocatalysts. *Chemsuschem* **2015**, *8*, 813–816. [\[CrossRef\]](#)
114. Iguchi, M.; Guan, C.; Huang, K.-W.; Kawanami, H. Solvent effects on high-pressure hydrogen gas generation by dehydrogenation of formic acid using ruthenium complexes. *Int. J. Hydrogen Energy* **2019**, *44*, 28507–28513. [\[CrossRef\]](#)
115. Iturmendi, A.; Rubio-Pérez, L.; Pérez-Torrente, J.J.; Iglesias, M.; Oro, L.A. Impact of Protic Ligands in the Ir-Catalyzed Dehydrogenation of Formic Acid in Water. *Organometallics* **2018**, *37*, 3611–3618. [\[CrossRef\]](#)
116. Luque-Gómez, A.; García-Abellán, S.; Munarriz, J.; Polo, V.; Passarelli, V.; Iglesias, M. Impact of Green Cosolvents on the Catalytic Dehydrogenation of Formic Acid: The Case of Iridium Catalysts Bearing NHC-phosphane Ligands. *Inorg. Chem.* **2021**, *60*, 15497–15508. [\[CrossRef\]](#)
117. Younas, M.; Rezakazemi, M.; Arbab, M.S.; Shah, J.; Rehman, W.U. Green hydrogen storage and delivery: Utilizing highly active homogeneous and heterogeneous catalysts for formic acid dehydrogenation. *Int. J. Hydrogen Energy* **2022**, *47*, 11694–11724. [\[CrossRef\]](#)
118. Curley, J.B.; Bernskoetter, W.H.; Hazari, N. Additive-Free Formic Acid Dehydrogenation Using a Pincer-Supported Iron Catalyst. *Chemcatchem* **2020**, *12*, 1934–1938. [\[CrossRef\]](#)
119. Celaje, J.J.A.; Lu, Z.; Kedzie, E.; Terrile, N.J.; Lo, J.N.; Williams, T.J. A prolific catalyst for dehydrogenation of neat formic acid. *Nat. Commun.* **2016**, *7*, 11308. [\[CrossRef\]](#) [\[PubMed\]](#)
120. Junge, H.; Boddien, A.; Capitta, F.; Loges, B.; Noyes, J.R.; Gladiali, S.; Beller, M. Improved hydrogen generation from formic acid. *Tetrahedron Lett.* **2009**, *50*, 1603–1606. [\[CrossRef\]](#)
121. Pfister, S.; Bayer, P.; Koehler, A.; Hellweg, S. Environmental Impacts of Water Use in Global Crop Production: Hotspots and Trade-Offs with Land Use. *Environ. Sci. Technol.* **2011**, *45*, 5761–5768. [\[CrossRef\]](#) [\[PubMed\]](#)
122. Matsunami, A.; Kayaki, Y.; Ikariya, T. Enhanced Hydrogen Generation from Formic Acid by Half-Sandwich Iridium(III) Complexes with Metal/NH Bifunctionality: A Pronounced Switch from Transfer Hydrogenation. *Chem. Eur. J.* **2015**, *21*, 13513–13517. [\[CrossRef\]](#)
123. Mellmann, D.; Barsch, E.; Bauer, M.; Grabow, K.; Boddien, A.; Kammer, A.; Sponholz, P.; Bentrup, U.; Jackstell, R.; Junge, H.; et al. Base-Free Non-Noble-Metal-Catalyzed Hydrogen Generation from Formic Acid: Scope and Mechanistic Insights. *Chem. Eur. J.* **2014**, *20*, 13589–13602. [\[CrossRef\]](#)
124. Montandon-Clerc, M.; Dalebrook, A.F.; Laurenczy, G. Quantitative aqueous phase formic acid dehydrogenation using iron(II) based catalysts. *J. Catal.* **2016**, *343*, 62–67. [\[CrossRef\]](#)
125. Picquet, M.; Tkatchenko, I.; Tommasi, I.; Wasserscheid, P.; Zimmermann, J. Ionic Liquids, 3. Synthesis and Utilisation of Protic Imidazolium Salts in Homogeneous Catalysis. *Adv. Synth. Catal.* **2003**, *345*, 959–962. [\[CrossRef\]](#)
126. Părvulescu, V.I.; Hardacre, C. Catalysis in Ionic Liquids. *Chem. Rev.* **2007**, *107*, 2615–2665. [\[CrossRef\]](#)
127. Berger, M.E.M.; Assenbaum, D.; Taccardi, N.; Spiecker, E.; Wasserscheid, P. Simple and recyclable ionic liquid based system for the selective decomposition of formic acid to hydrogen and carbon dioxide. *Green Chem.* **2011**, *13*, 1411–1415. [\[CrossRef\]](#)
128. Yasaka, Y.; Wakai, C.; Matubayasi, N.; Nakahara, M. Slowdown of H/D Exchange Reaction Rate and Water Dynamics in Ionic Liquids: Deactivation of Solitary Water Solvated by Small Anions in 1-Butyl-3-Methyl-Imidazolium Chloride. *J. Phys. Chem. A* **2007**, *111*, 541–543. [\[CrossRef\]](#)
129. Anderson, J.L.; Ding, J.; Welton, T.; Armstrong, D.W. Characterizing Ionic Liquids On the Basis of Multiple Solvation Interactions. *J. Am. Chem. Soc.* **2002**, *124*, 14247–14254. [\[CrossRef\]](#)

130. Yasaka, Y.; Wakai, C.; Matubayasi, N.; Nakahara, M. Controlling the Equilibrium of Formic Acid with Hydrogen and Carbon Dioxide Using Ionic Liquid. *J. Phys. Chem. A* **2010**, *114*, 3510–3515. [CrossRef]
131. Bates, E.D.; Mayton, R.D.; Ntai, I.; Davis, J.H. CO₂ Capture by a Task-Specific Ionic Liquid. *J. Am. Chem. Soc.* **2002**, *124*, 926–927. [CrossRef]
132. Zhang, Z.; Xie, Y.; Li, W.; Hu, S.; Song, J.; Jiang, T.; Han, B. Hydrogenation of Carbon Dioxide is Promoted by a Task-Specific Ionic Liquid. *Angew. Chem.* **2008**, *120*, 1143–1145. [CrossRef]
133. Scholten, J.D.; Precht, M.H.G.; Dupont, J. Decomposition of Formic Acid Catalyzed by a Phosphine-Free Ruthenium Complex in a Task-Specific Ionic Liquid. *Chemcatchem* **2010**, *2*, 1265–1270. [CrossRef]
134. Geldbach, T.J.; Dyson, P.J. A Versatile Ruthenium Precursor for Biphasic Catalysis and Its Application in Ionic Liquid Biphasic Transfer Hydrogenation: Conventional vs Task-Specific Catalysts. *J. Am. Chem. Soc.* **2004**, *126*, 8114–8115. [CrossRef]
135. Baaqel, H.; Tulus, V.; Chachuat, B.; Guillén-Gosálbez, G.; Hallett, J. Uncovering the True Cost of Ionic Liquids using Monetization. In *Computer Aided Chemical Engineering*; Elsevier: Amsterdam, The Netherlands, 2020; Volume 48, pp. 1825–1830. [CrossRef]
136. The Cost of Water and Its Pricing General Principles. Available online: <https://wikiwater.fr/the-cost-of-water-and-its-pricing> (accessed on 27 November 2022).
137. Onishi, N.; Kanega, R.; Kawanami, H.; Himeda, Y. Recent Progress in Homogeneous Catalytic Dehydrogenation of Formic Acid. *Molecules* **2022**, *27*, 455. [CrossRef]
138. Leon, A. *Hydrogen Technology: Mobile and Portable Applications*; Springer: Berlin/Heidelberg, Germany, 2008.
139. Lewis, N.S.; Nocera, D.G. Powering the planet: Chemical challenges in solar energy utilization. *Proc. Natl. Acad. Sci. USA* **2006**, *103*, 15729–15735. [CrossRef]
140. Whitesides, G.M.; Crabtree, G.W. Don't Forget Long-Term Fundamental Research in Energy. *Science* **2007**, *315*, 796–798. [CrossRef]
141. Gao, Y.; Kuncheria, J.K.; Jenkins, H.A.; Puddephatt, R.J.; Yap, G.P.A. The interconversion of formic acid and hydrogen/carbon dioxide using a binuclear ruthenium complex catalyst. *J. Chem. Soc. Dalton Trans.* **2000**, 3212–3217. [CrossRef]
142. Dicks, A.L.; Rand, D.A.J. *Fuel Cell Systems Explained*, 3rd ed.; Wiley: Hoboken, NJ, USA, 2018. [CrossRef]
143. Czaun, M.; Kothandaraman, J.; Goeppert, A.; Yang, B.; Greenberg, S.; May, R.B.; Olah, G.A.; Prakash, G.K.S. Iridium-Catalyzed Continuous Hydrogen Generation from Formic Acid and Its Subsequent Utilization in a Fuel Cell: Toward a Carbon Neutral Chemical Energy Storage. *ACS Catal.* **2016**, *6*, 7475–7484. [CrossRef]
144. Hydrozine, Liquid Organic Hydrogen Carrier. Available online: <https://www.dens.one/> (accessed on 21 October 2022).
145. Satyapal, S.; U.S. Department of Energy, (DoE). Hydrogen and Fuel Cell Technologies Office, 2021 AMR Plenary Session. Available online: https://www.hydrogen.energy.gov/pdfs/review21/plenary5_satyapal_2021_o.pdf (accessed on 3 January 2023).
146. Kayfeci, M.; Keçebaş, A.; Bayat, M. Hydrogen production. In *Solar Hydrogen Production*; Elsevier: Amsterdam, The Netherlands, 2019; pp. 45–83. [CrossRef]
147. Ruth, M.; Jadun, P.; Gilroy, N.; Connelly, E.; Boardman, R.; Simon, A.J.; Elgowainy, A.; Zuboy, J. The Technical and Economic Potential of the H₂@Scale Hydrogen Concept within the United States. 2020. Available online: <https://www.nrel.gov/docs/fy21osti/77610.pdf> (accessed on 4 January 2023).
148. IEA. The Future of Hydrogen, Seizing Today's Opportunities, Report Prepared by the IEA for the G20, Japan. June 2019. Available online: https://iea.blob.core.windows.net/assets/9e3a3493-b9a6-4b7d-b499-7ca48e357561/The_Future_of_Hydrogen.pdf (accessed on 6 January 2023).
149. Stathi, P.; Deligiannakis, Y.; Avgouropoulos, G.; Louludi, M. Efficient H₂ production from formic acid by a supported iron catalyst on silica. *Appl. Catal. A Gen.* **2015**, *498*, 176–184. [CrossRef]
150. Ahn, Y.; Byun, J.; Kim, D.; Kim, B.-S.; Lee, C.-S.; Han, J. System-level analysis and life cycle assessment of CO₂ and fossil-based formic acid strategies. *Green Chem.* **2019**, *21*, 3442–3455. [CrossRef]

Disclaimer/Publisher's Note: The statements, opinions and data contained in all publications are solely those of the individual author(s) and contributor(s) and not of MDPI and/or the editor(s). MDPI and/or the editor(s) disclaim responsibility for any injury to people or property resulting from any ideas, methods, instructions or products referred to in the content.